ISTANBUL TECHNICAL UNIVERSITY ★ FACULTY OF AERONAUTICS AND ASTRONAUTICS

UNMANNED AERIAL VEHICLE WING DESIGN AND STRUCTURAL ANALYSIS

GRADUATION PROJECT

Burak BAYRAM

Department of Aeronautical Engineering(100 %Eng.)

Thesis Advisor: Asst. Prof. Dr. Hayri ACAR

JANUARY, 2022

ISTANBUL TECHNICAL UNIVERSITY ★ FACULTY OF AERONAUTICS AND ASTRONAUTICS

UNMANNED AERIAL VEHICLE WING DESIGN AND STRUCTURAL ANALYSIS

GRADUATION PROJECT

Burak BAYRAM
110100062

Department of Aeronautıcal Engineering(100 %Eng.)

Thesis Advisor: Asst. Prof. Dr. Hayri ACAR

JANUARY, 2022

Burak BAYRAM,student of ITU Faculty of Aeronautics and Astronautics student ID **110100062**, successfully defended the **graduation** entitled "**UNMANNED AERIAL VEHICLE WING DESIGN AND STRUCTURAL ANALYSIS**", which he prepared after fulfilling the requirements specified in the associated legislations, before the jury whose signatures are below.

Thesis Advisor :	**Asst. Prof. Dr. Name SURNAME** İstanbul Technical University	Hayri ACAR
Jury Members :	**Prof. Dr. Name SURNAME** İstanbul Technical University	.....
	Prof. Dr. Name SURNAME İstanbul Technical University	.....
	Prof. Dr. Name SURNAME İstanbul Technical University	.....

Date of Submission : 17 January 2022
Date of Defense : 31 January 2022

To my family,

FOREWORD

I would like to thank my mentor Asst. Prof. Dr. Hayri ACAR, who helped me do my graduation work and did not spare his support.
I would also like to thank Bias Engineering and PE Erman YAYLAĞAN for introducing me to the world of analysis and educating me in the field.
In addition, I would like to thank my family and friends who have not spared their financial and moral support from me for a moment in all the difficult processes I have been going through during my education life.

January 2022 Burak BAYRAM

TABLE OF CONTENTS

Page

FOREWORD ..... **v**
TABLE OF CONTENTS ..... **vvii**
ABBREVIATIONS ..... **ix**
LIST OF TABLES ..... **xx**
LIST OF FIGURES ..... **xi**
SUMMARY ..... **xxii**
1. INTRODUCTION **13**
1.1 Purpose of Thesis 13
1.2 Literature Review 14
2. STRUCTURAL DESIGN **18**
2.1 Wing Geometry 18
2.1.1 Wingspan and Maximum Take-off Weight 18
2.1.2 Aspect Ratio and Wing Area 19
2.1.3 Determination of Taper Ratio and Chord Length 20
2.1.4 Sweep Angle 21
2.1.5 Dihedral Angle 21
2.2 Determination of Thickness Ratio and Wing Profile 218
3. MODELIN OF THE WING **29**
3.1 Determination of Spar Structure 31
3.1.1 Determination of the Number, Location, and Structure of the Spar 31
3.2 Determination of Rib Structure ..... 3**Error! Bookmark not defined.**
3.3 Determination of Shell Structure 34
4. LOADS AFFECTING THE WING **35**
4.1 Structural Loads Acting on the Wing 35
4.2 Aerodynamic Loads Acting on the Wing 36
4.2.1 Safety Factor 37
4.2.2.Load Factor 37
4.3 Calculation of the Lift Force Required 38
4.4 Calculation of the Maximum Load 39
4.4.1 Empty Weight Calculation 40
4.4.2 Weight Calculation of the Camera System and the Warhead 41
5. ANALYSIS **41**
5.1 Static Analysis of the Designed Wing 41
5.1.2 Determining the Lift Distribution on the Wing 43
5.1.3 Creating Mesh Network 45
5.1.4 Wing Material Selection 47
5.1.5 Thickness of Wing Selection 47
REFERENCES **48**

ABBREVIATIONS

UAV	**:** Unmanned Aerial Vehicle
MTOW	**:** Maximum Take-off Weight
REF	**:** Reference
AR	**:** Aspect Ratio
NACA	**:** National Advisory Committee for Aeronautics
CFRP	**:** Carbon Fiber Reinforced Polymer

LIST OF TABLES

Page

Table 1.1 : Technical Characteristics of Similar Aircraft 15
Table 2.1 : Wing Design Parameters..... 29
Table3.1 : Maximum Load and Lift Forces. 39
Table 4.1: Empty Weight Fraction with W_0 40
Table 5.1 : Detailed Lift Distribution on The Wing..... 43
Table 5.2 : Carbon Fiber Material Properties..... 47

LIST OF FIGURES

Page

Figure 1.1 : Isometric View of The Sample Design of Fixed-Wing UAVs..... 14
Figure 1.2 : Bayraktar Mini UAV. 16
Figure 1.3 : Leleka-100 UAV. 16
Figure 1.4 : Avian-S UAV. 17
Figure 2.1 : UAV Wing Span and Weight. 19
Figure 2.2 : Aspect Ratio Calculation of Rectangular Wing 19
Figure 2.3 : Wing Taper Ratio. 20
Error! Reference source not found.Error! Reference source not found...... 21
Error! Reference source not found.Error! Reference source not found...... 22
Error! Reference source not found.Error! Reference source not found...... 23
Figure 2.7 : Comparison of Profiles …..... 24
Figure 2.8 : Representation of The Thickness to Chord Ratio (t/c). 24
Figure 2.9 : Graph of the lift coefficient C_l vs Angle of attack α. 25
Figure 2.10 : Graph of the drag coefficient C_d vs Angle of attack α. 26
Figure 2.11 : Graph of the lift coefficient C_l and Drag coefficient C_d 27
Figure 2.12 : Graph of the pitching moment coefficient C_m vs Angle of attack α ... 28
Figure 3.1 : Wing Skeleton Structure Sample 29
Figure 3.2 : Wing Top View 30
Figure 3.3 : Side View of the Wing 30
Figure 3.4 : Isometric View of the Wing. 31
Figure 3.5 : Isomteric View of the Spar Profile. 32
Figure 3.6 : Lateral View of the Rib Structure. 33
Figure 3.7 : Isometric View of the Rib Structure 33
Figure 3.8 : Isometric View of the Shell Structure 34
Figure 3.9 : Wing Structure Designed Together with Shell, Rib, and Spar..... 35
Figure 4.1 : Structural Loads Acting on the Wing 36
Figure 4.2 : Aerodynamic Force Vectors on An Airfoil 37
Figure 4.3 : V-n Diagram 38
Figure 5.1 : Lift Distribution over One Wing 44
Figure 5.2 : Lift Force Distribution over Ribs 44
Figure 5.3 : Mesh Network for Shell 45
Figure 5.4 : Mesh Network for Spars 46
Figure 5.5 : Mesh Network for Ribs 46

UNMANNED AERIAL VEHICLE WING DESIGN AND STRUCTURAL ANALYSIS

SUMMARY

One of the most popular aviation applications today is UAVs. UAVs can be used in various observation, intelligence, offensive, suicide missions and they can be controlled remotely. For these reasons, it is also aimed to make a design of the wing structure, which is one of the most important parts of a mini-unmanned aerial vehicle, and structural analysis of the design made in this finishing work.

Unmanned aerial vehicles are vehicles that must be cruising for a long time, as they can perform long-term tasks such as observation and intelligence without a human factor. During this course, it is very important for unmanned aerial vehicles to be able to perform their assigned tasks so that the aircraft can maintain its structural integrity and fly in the most efficient way possible.

The study was started by conducting a comprehensive literature survey on mini-unmanned aerial vehicles. In the literature review, it was noted that the UAV type that is the subject of the study has compact small dimensions and is lightweight in accordance with the transportation of military personnel on the ground. First, the technical characteristics of UAVs designed for observation, intelligence, and suicide missions were tabulated and the average value of these technical characteristics was determined. Considering these average values, an efficient wing design was aimed at. 3 different airfoils used in similar aircraft have been determined and based on the critical values of these profiles, the airfoil that will provide the most lifting force has been selected. In addition, important design parameters such as wingspan, tapering ratio, arrow angle were also determined. The SOLIDWORKS program was used to model the wing with three-dimensional drawings, where the airfoil profile and other design dimensions were determined, and then linear static and modal structural analyses were performed with the MSC PATRAN/NASTRAN program, a package program using the Finite Element Method.

In accordance with these analyzes applied to a designed mini-unmanned aerial vehicle wing, a report was prepared and the study was completed by observing that the carrying ability and strength of the wing were sufficient.

1. INTRODUCTION

One of the most important, most modern, and most remarkable aviation applications of today's era is Unmanned Aerial Vehicles. UAVs are actively used all over the world for many purposes such as observation, reconnaissance, destruction, transportation, agricultural spraying, camera shooting, fire fighting. In recent years, Turkey has been one of the leading countries in the world in terms of UAVs performing observation, intelligence, offensive, and suicide missions, which has been instrumental in making the graduation project on UAVs. The most critical structural element of any aircraft on Earth is the wings of that aircraft. The wings not only provide the aircraft with the lift force they provide but also provide the maneuverability and stability they need for the aircraft. For this reason, the most important design and analysis studies performed on an aircraft are those performed on the wing. Since the wings encounter many forces that they must carry during the flight, these designs and analyzes must be carried out very carefully. Therefore, longer operation times, as much agility as possible, and high cruising speed are important elements for UAVs. UAVs that can be used both manually and autonomously reduce the risk that may occur and can fly in adverse conditions. In this study, small unmanned aerial vehicles used today were investigated and the characteristic features of aircraft designed for similar tasks were determined. According to these characteristics, the wing design was made and supported by theoretical analyses.

1.1 Purpose of Thesis

The main purpose of the thesis is to design a UAV wing with optimum values and to perform stress, deformation, and vibration analysis of this wing with the MSC PATRAN/NASTRAN Package Program using the finite element method. During these stages, the types of UAVs that have already been produced and are actively used, which do not exceed 10 kg in weight, have been studied and, as a result of these reviews, the “Mini” type UAV has been selected for the design. The initial parameters were taken from these types of UAVs and the design was started with these values. After optimization studies using the initial values, the design of the wing was completed. Then, studies were carried out to ensure that the wing was very small and light, while at the same time being high-performance. When carrying out these designs, attention was

paid to the parameters of weight, portability, and ease of production. After the structural design was completed with the 'SOLIDWORKS' program, the necessary analyses were carried out using FEM with the “MSC PATRAN/NASTRAN” package program.

1.2 Literature Review

Mini-UAVs, which are designed for military use at most for the purpose of use, have a low payload weight due to the fact that they are small. For this reason, since missiles and weapons systems cannot be placed in a military sense, they are usually used for reconnaissance and observation in border areas, as well as for suicide purposes. The most important part of a fixed-wing aircraft is the wings that provide lift and control. As a wing design, it is the location of the wing that should be planned first. When looking at previously designed mini-unmanned aerial vehicles, the wing position is located above the fuselage. In mini-UAVs flying at low speeds, thick wing profiles were preferred when choosing a wing profile.

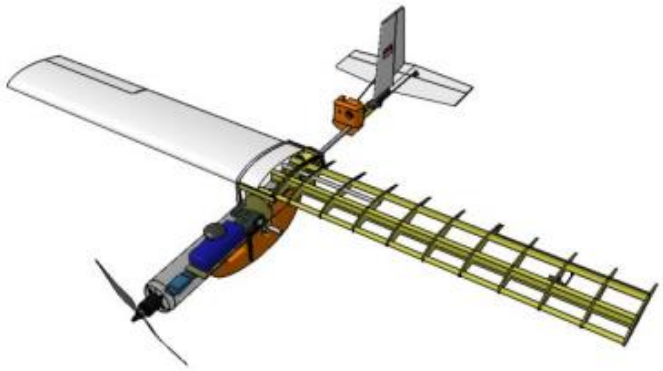

Figure 1.1 : Isometric View of The Sample Design of Fixed-Wing UAV.

25 mini-unmanned aerial vehicles, mostly used for similar reconnaissance, surveillance, offensive, suicide missions, have been studied. The technical characteristics of the mini UAV not exceeding 10 kg of weight to be used within the scope of this study are tabulated and the average values are shown.

Table 1.1 : Technical Characteristics of Similar Aircraft.

	NAME	MTOW (kg)	WINGSPAN (m)	CRUISE SPEED (km/h)	MAX SPEED (km/h)	SERVICE CEILING (ft)	CRUISE CEILING (ft)	REF.
1	BAYRAKTAR MINI	3,50	2,00	55,56	74,08	4000,00	2000	[1]
2	ALPAGU	1,90	1,25	92,60	120,38	None	400,00	[2]
3	ASELSAN MIUS	8,00	3,00	45,00	130,00	16404,19	None	[3]
4	GLOBIHA	3,10	1,51	65,00	110,00	457,20	None	[4]
5	TAI KEKLIK	10,00	1,61	120,00	150,00	6889,76	None	[5]
6	RAM UAV	8,00	2,30	70,00	150,00	None	None	[6]
7	LELEKA-100	5,40	2,00	60,00	80,00	4921,25	3280,83	[7]
8	UA BETA	4,50	None	75,00	None	9842,51	4921,25	[8]
9	A1-CM FURIA	5,50	2,00	65,00	130,00	6889,76	None	[9]
10	ALBATROSS	10,00	3,00	68,00	129,00	None	None	[10]
11	SKATE SUAS	1,20	0,61	37,04	92,60	14000,00	500	[11]
12	SWITCHBLADE 300	2,50	None	101,39	160,93	15000,00	500	[12]
13	RQ-11 RAVEN	1,90	1,40	32,00	81,00	14000,00	500	[13]
14	DRAGON EYE RQ-14/A	2,70	1,14	65,00	35,00	1000,00	None	[14]
15	DESERT HAWK III	4,00	1,37	46,30	92,60	492,12	None	[15]
16	SKYLARK I-LEX	7,50	3,00	None	None	15000,00	None	[16]
17	RAFAEL SKYLITE B	6,00	1,50	126,00	79,20	984,25	328,08	[17]
18	AVIAN-S	4,50	1,60	81,00	63,00	13000,00	None	[18]
19	PTERYX	5,00	2,80	160,00	120,00	9842,51	1706,03	[19]
20	LEHMANN LA300	0,95	0,92	20,00	80,00	1640,41	65,61	[20]
21	TRACKER 120	8,70	3,30	25,00	None	8202,02	None	[21]
22	EMT ALADIN	4,00	1,46	45,00	90,00	14764,00	656,16	[22]
23	TOPCON SIRIUS	2,70	1,63	65,00	None	8530,18	2460,92	[23]
24	ZALA 421-08M	2,50	0,81	130,00	65,00	16404,19	None	[24]
25	ZALA 421-16E2	7,50	2,80	110,00	65,00	16404,19	None	[25]
	MEAN	**4,86**	**1,87**	**73,32875**	**99,89**	**9030,39**	**1443,24**	

The take-off method of the sample UAVs in the table is catapult/hand launched. The electric motor type is preferred in all of them. The type of wing is densely rectangular and the type of

wing is tapered. The flight preparation and installation time is under 10 minutes in total. The average payload is 1.55 kg, the average flight time is 95.58 min, and the average range is 38.63 km. Considering the average values, the 3 mini-UAVs closest to the projected design can be listed in the following ways.

Figure 1.2 : Bayraktar Mini UAV

Figure 1.3 : Leleka-100 UAV

Figure 1.4 : Avian-S UAV

2. STRUCTURAL DESIGN

2.1 Wing Geometry

The wing geometry is very important for both flight efficiency and structural strength. Various wing geometries are available on aircraft designed for different purposes. For example, the delta wing type is used for military aircraft flying at above-sound speeds, while wings with a large wing area are designed for subsonic commercial aircraft. Aircraft that will fly in low Reynolds numbers, such as unmanned aerial vehicles, prefer a high aspect ratio and a rectangular wing. It is known that wings of an elliptical shape are the most efficient type of wings in subsonic flights. But considering the ease of manufacturing, the rectangular wing type was considered suitable.

2.1.1 Wingspan and Maximum Take-off Weight

The parameter that we evaluate as the wingspan is a parameter that has an effect on the lifting force and drag forces, indicating the distance from one end of the wing to the other end. However, the parameter that we consider as the maximum take-off weight refers to the maximum weight that an aircraft can have during take-off, while it is an important parameter that affects the lifting force that must be generated. When determining these two parameters, they cannot be determined independently of each other. When determining these two parameters, the arithmetic mean of the values of 25 similar reference aircraft was taken, as well as other parameters. These values are 1.87 meters and 4.86 kilograms. It can be confirmed the accuracy of these elections from Figure 2.1.[30] The x-axis of the graph refers to the wingspan values in meters, while the y-axis refers to the total weight. The accuracy of the selected parameters is observed when the point corresponding to the selected values is marked. As a result, it can be used 1.87 meters as the wingspan for now and 4.86 kilograms as the maximum take-off weight.

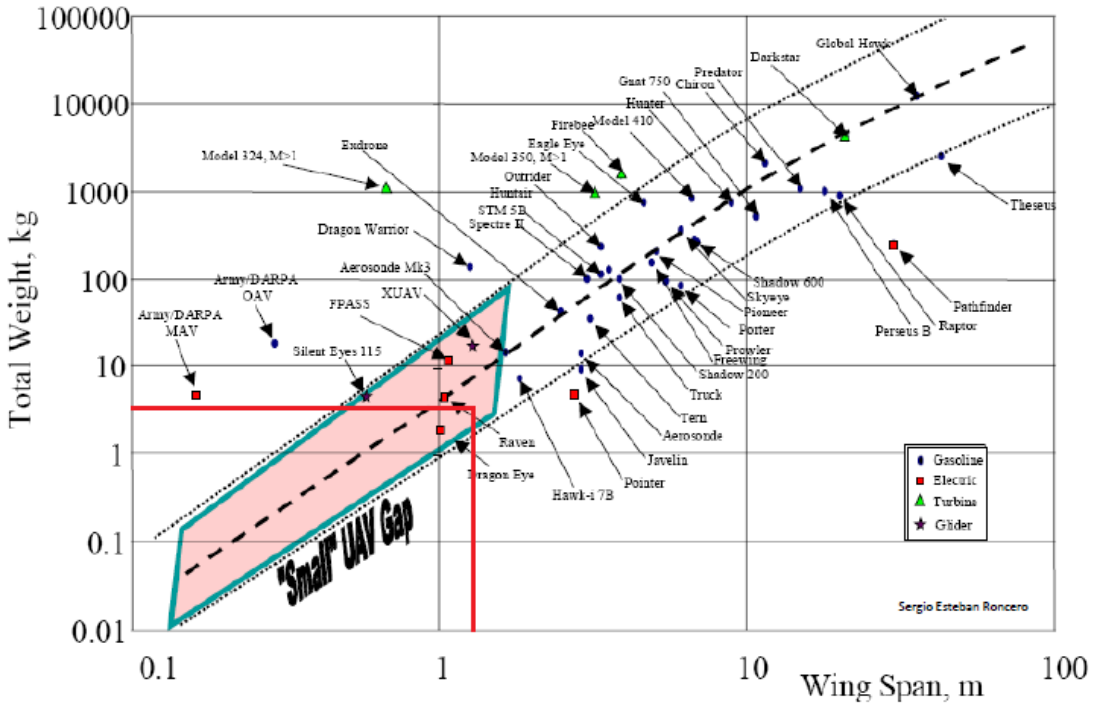

Figure 2.1 : UAV Wing Span and Weight.

2.1.2 Aspect Ratio and Wing Area

The aspect ratio should be kept high in aircraft flying at subsonic speeds and planned to stay in the air for a long time. In the study conducted by Kontogiannis, the aspect ratio for the wing geometry of a designed mini UAV was determined to be 10. [28] Thus, a chord length of 0.187 m is obtained despite a wingspan of 1.87 m.

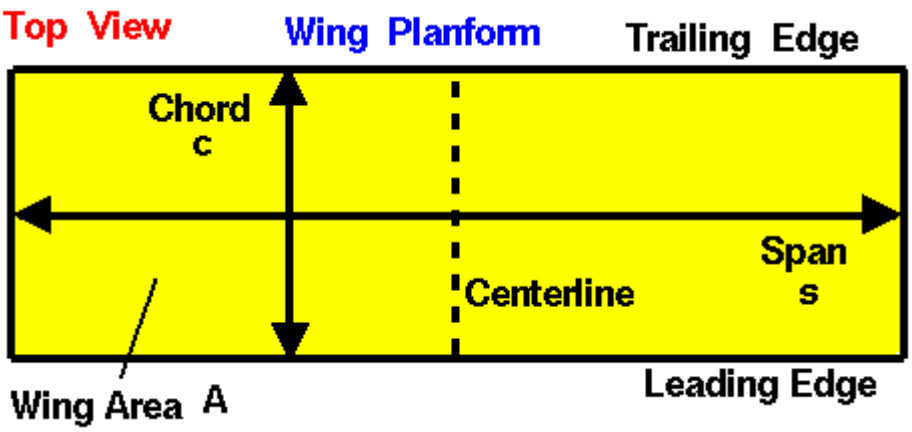

Figure 2.2 : Aspect Ratio Calculation of Rectangular Wing.

$$Aspect\ Ratio\ AR = 10 = \frac{S^2}{A} = \frac{S^2}{s*c_{mean}} = S/c_{mean} = \frac{1.87}{c_{mean}}$$

$$Mean\ Chord\ Lenght\ c_{mean} = 0.187\ m$$

2.1.3 Determination of Taper Ratio and Chord Length

The ratio of the chord length at the end of the wing to the chord length at the part of the wing called the root where it merges with the airframe is called the taper ratio. Elliptical wings have the lowest induced drag compared to other wing types, while rectangular wings have more induced drag compared to elliptical wings. [29] Despite this, elliptical wings are a rather difficult process to produce, while rectangular wings are quite easy. It is because of this advantage of the ease of manufacture that the rectangular wing was chosen. In other words, the chord length of the wing at the root and the chord length at the tip are equal to each other. As a result, the wing taper ratio was considered to be "1".

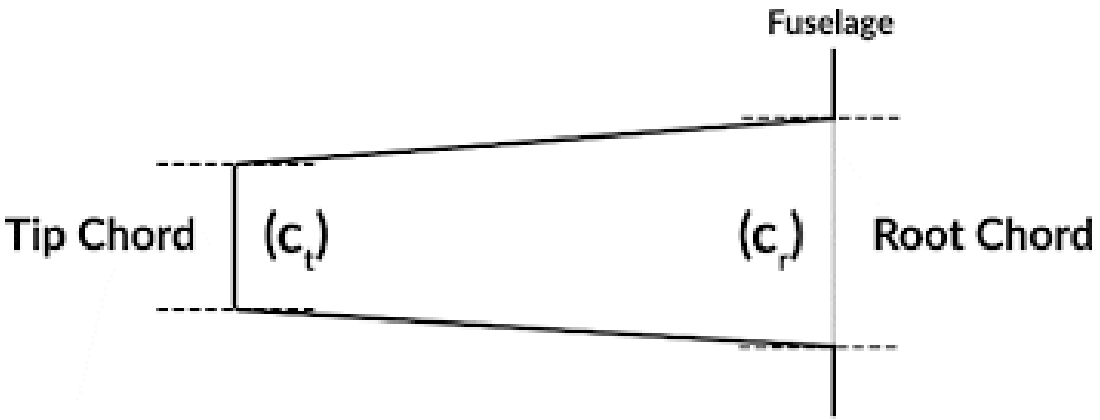

Figure 2.3 : Wing Taper Ratio

$$Taper\ ratio = \frac{c_t}{c_r} = 1$$

$$c_{mean} = \frac{c_t + c_r}{2} = 0.187m$$

$$c_t = c_r = 0.187m$$

2.1.4 Sweep Angle

The sweep angle is called the angle that the wing makes with the fuselage when the aircraft is viewed from above. The sweep angle is very important for aircraft that reach high speeds. The sweep angle increases the critical Mach number in commercial aircraft and allows the aircraft to reach higher speeds. In military aircraft, the sweep angle should be kept very high because the sound wall should be exceeded. Since using a sweep-angle wing in our unmanned aerial vehicle, which will fly at low speed and low altitude, will reduce flight efficiency and reduce lift, it is necessary to use a sweep angle of 0 degrees.

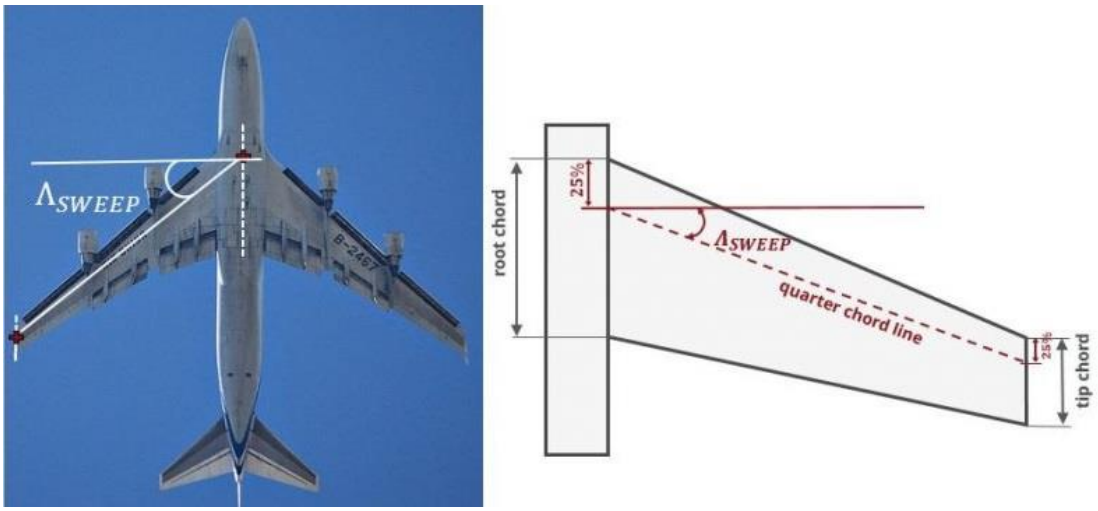

Figure 2.4 : Sweep Angle

2.1.5 Dihedral Angle

The angle that the wings of airplanes make with the horizontal is called the dihedral angle. It is used to increase the rotational stability of the aircraft [26]. The dihedral angle, which has a great influence on decisiveness, is between 0-2 degrees on subsonic flying wings without sweep angle, while it is set at 0 degrees considering ease of manufacture and material flexibility.

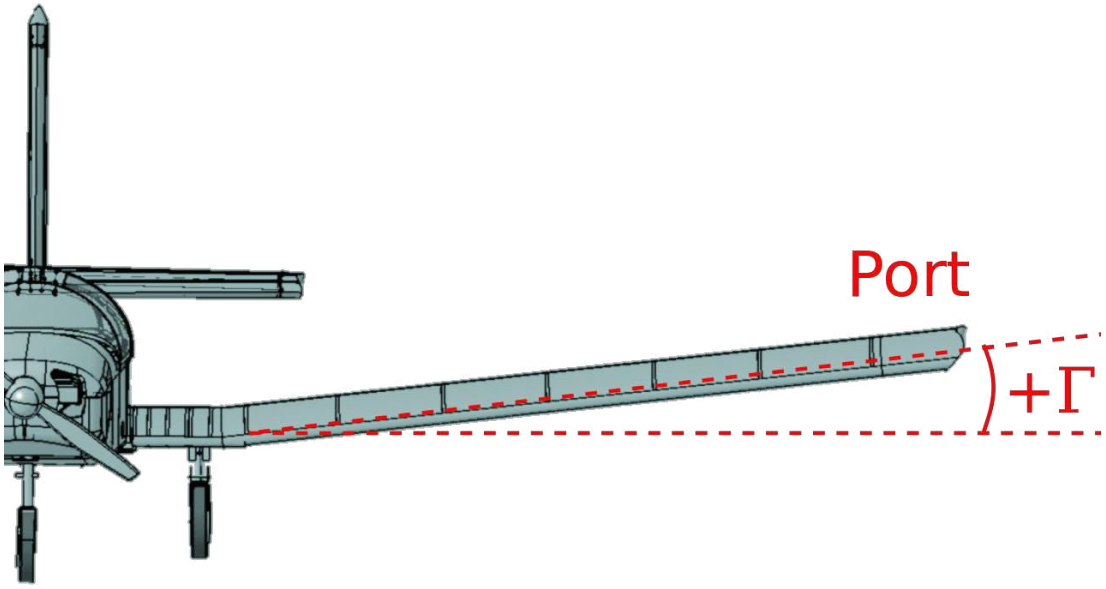

Figure 2.5 : Dihedral Angle

2.2. Determination of Thickness Ratio and Wing Profile

Wing profiles are generally divided into 3 main groups: fat, thin, and very thin. Profiles with a thickness ratio of more than 14% are called a fat profile, those with a thickness between 6 and 14 percent are called a thin profile, and profiles with a thickness below 6 percent are also called a very thin profile. Dec Thin profile is also called a very thin profile. [26] In NACA profiles, the last two figures indicate the thickness ratio of the wing. The airfoil is the most important parameter that determines the performance and flight characteristics of an aircraft. The airfoil, which will be selected by the flight performance and requirements, determines the cruising speed, take-off, and landing distances, stall angle, and aerodynamic efficiency. It is desirable that the drag coefficient is quite low and the transport coefficient is large. In addition, the choice of profile is also very effective on stability. Since the average service ceiling value of similar aircraft is about 9000 ft (2750 m), the wing profile of a mini-unmanned aerial vehicle should have a minimum drag coefficient (CD) and a maximum transport coefficient (CL) for low Reynolds numbers. In order to choose the most suitable airfoil, more than one airfoil should be evaluated and the one that is suitable for performance should be selected. The equivalent of the average cruise speed and maximum speed values as the number of mach are used to determine the design hump ratio December.[26] The cruising speed of our aircraft is low–speed, as it is in the Mach band of 0.0598 - 0.0813. The graph given below shows the

thickness ratio according to the number of Mach. According to this graph, the thickness ratio can be determined approximately as 15% -15.6%. Considering that the speed of our aircraft is low and that aircraft at this speed use fat wing profiles in their wing profiles and that the thickness ratio of these profiles is greater than 14%, we will have seen both the speed values of the aircraft and the accuracy of the thickness ratio.[26]

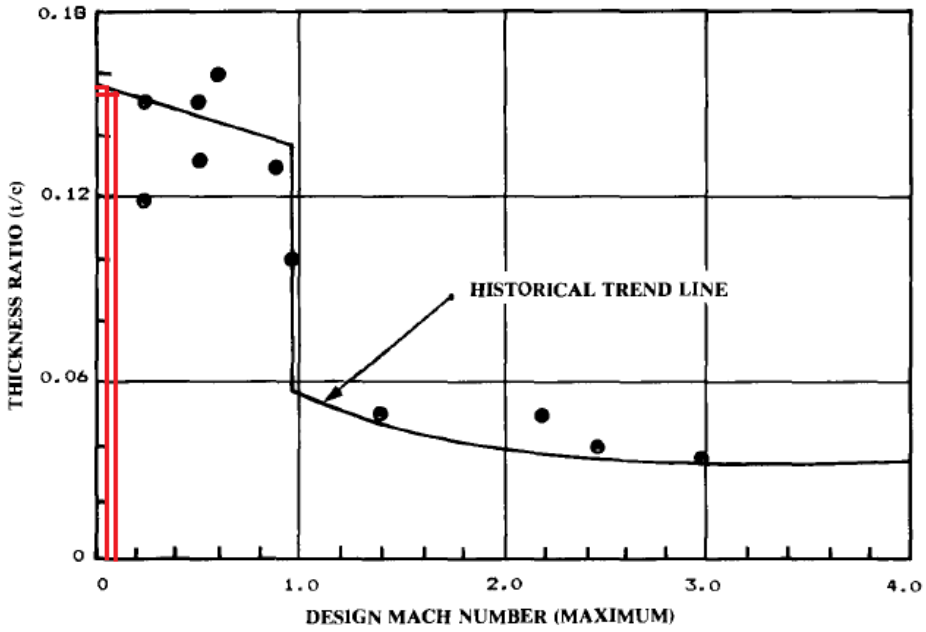

Figure 2.6 : Thickness Ratio Historical Trend.

The NACA 4 digit airfoil series, which is in the desired thickness to chord ratio range and is relatively easier and stable to manufacture, has been reviewed on the airfoiltools.com website. As a result, 3 reference profiles were obtained. [27] Reference profiles NACA0015, NACA2415 and NACA4415 are compared in the XFLR5 program.

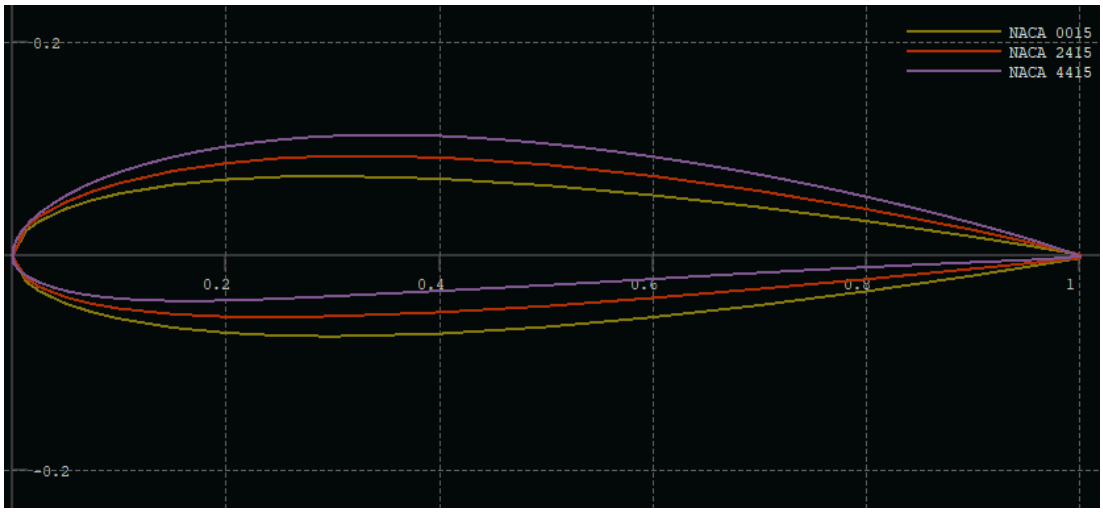

Figure 2.7 : Comparison of Profiles.

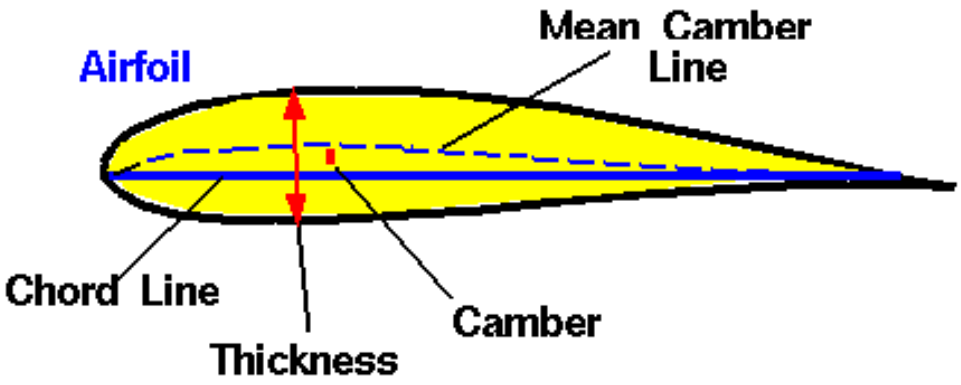

Figure 2.8 : Representation of The Thickness to Chord Ratio (t/c).

$$V_{cruise} = Cruising\ Velocity$$

$$V_{max} = Maximum\ Maneuver\ Velocity$$

$$Mach = Mach\ number = \frac{Velocity}{Speed\ of\ Sound}$$

$$\frac{t}{c} = Thickness\ to\ Chord\ Ratio$$

$$V_{cruise} = 73.32\ kmh < V < V_{max} = 98.99\ kmh$$

$$Mach_{min} = 0.0598 < V < Mach_{max} = 0.0813$$

$$\left(\frac{t}{c}\right)_{min} = 0.15 < \frac{t}{c} < \left(\frac{t}{c}\right)_{max} = 0.156$$

Considering the average values of similar unmanned aerial vehicles, the maximum Reynolds number Re_{max} is calculated as follows, taking into account the maximum speed, ceiling height, and wing dimensions. The maximum flight speed V_{max}, chord length c, the dynamic viscosity of air μ at maximum altitude and the air density ρ are taken as $27.7472\frac{m}{s}$, $0.187\ m$, $1.6379e-5\ Ns/m2$, $0.7380\ kg/m^3$, respectively[29]:

$$Re_{max} = (\rho V_{max} c)/\mu = (0.738*27.7472*0.187)/(1.6379e-5) = 233792.2244$$

The lift, drag, and pitch moment coefficients were analyzed in the XFLR5 program using the determined Reynolds number. For certain wing profiles the change of the coefficients mentioned with the angle of attack, which varies between -10 degrees and +15 degrees, is shown in the graphs below.

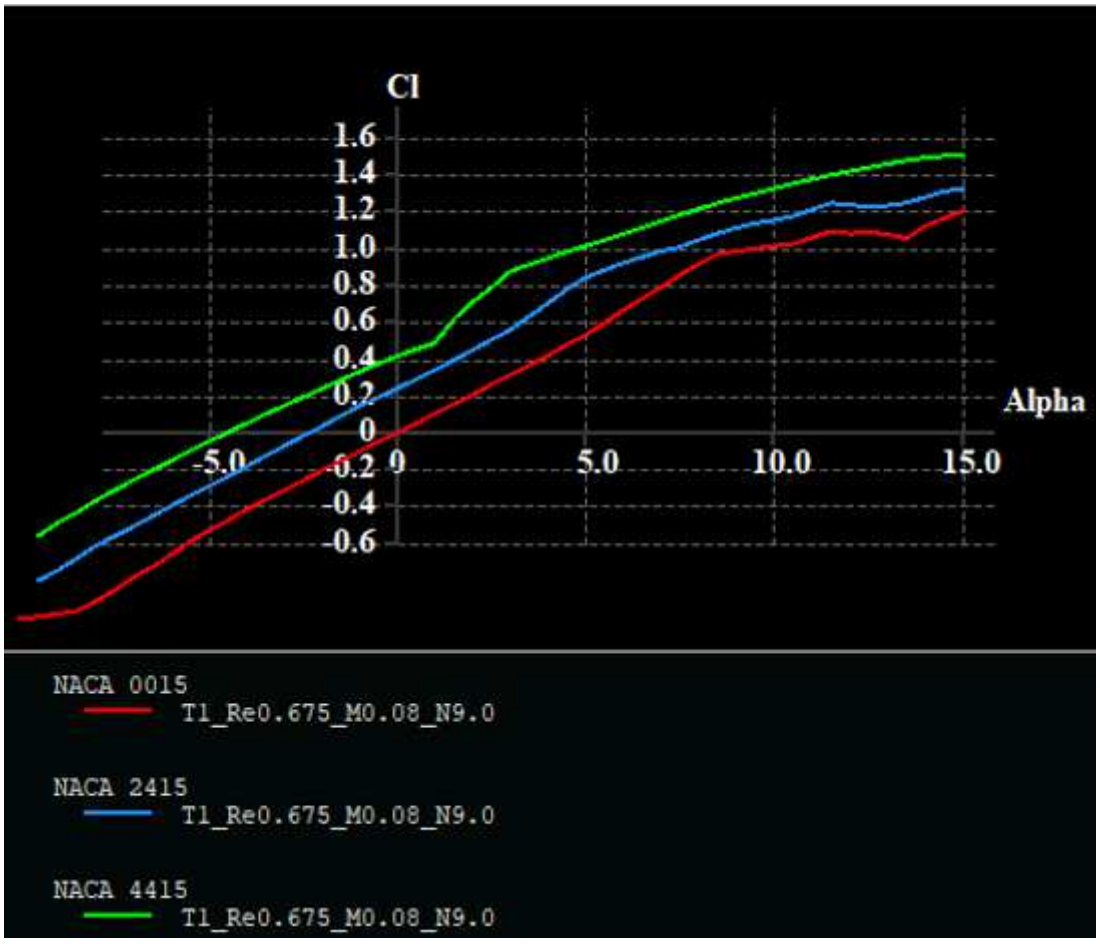

Figure 2.9: Graph of the lift coefficient C_l vs Angle of attack α.

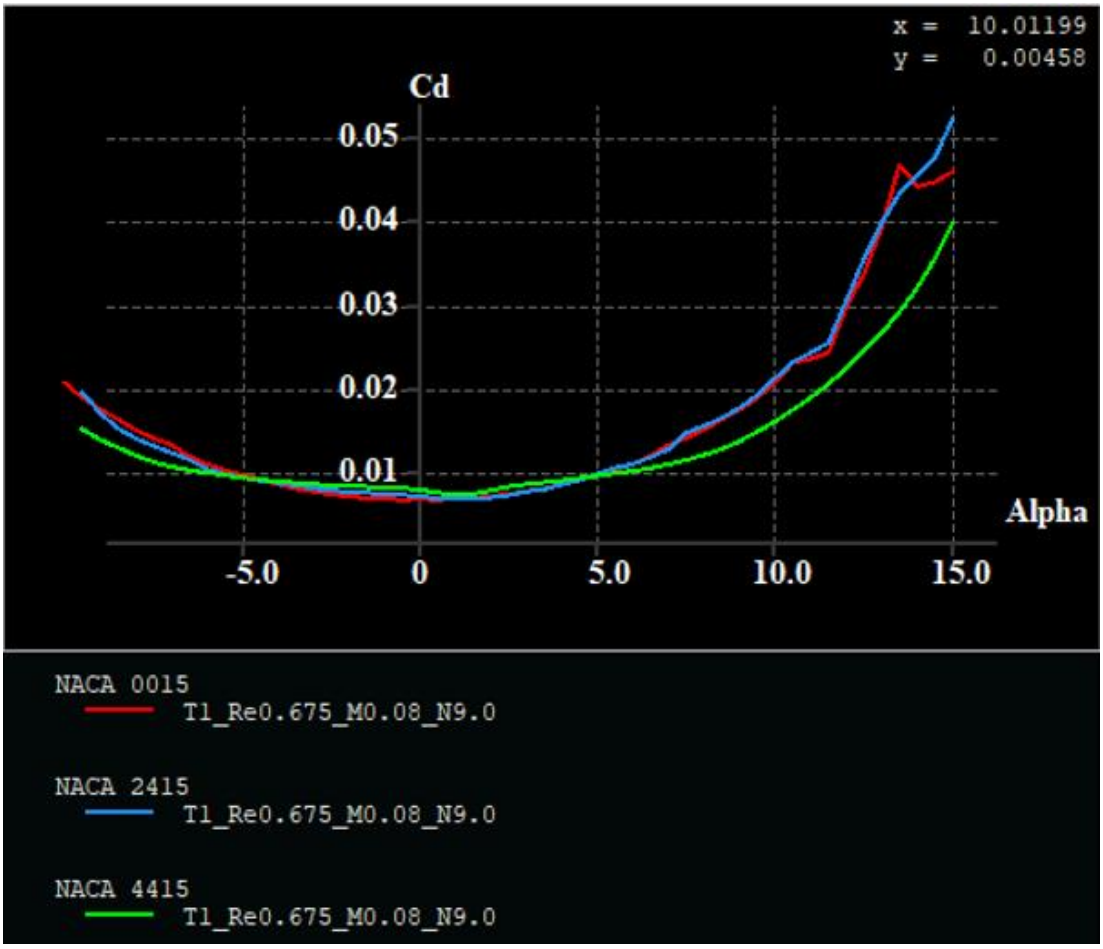

Figure 2.10: Graph of the drag coefficient C_d vs Angle of attack α.

It seems that the best value for the angle of attack of the lift coefficient and the drag coefficient belongs to NACA4415. At the same time, considering that an unmanned aerial vehicle can perform fast maneuvers, the stall angle is also important for us. The wing profile, where the stall angle is also the highest, again belongs to the NACA4415 profile. With this analysis, the NACA4415 profile can be preferred both because it provides the highest lifting force and because it can be reached at high angles of attack.

The following graph shows the variation of the lift coefficient with the varying drag coefficient.

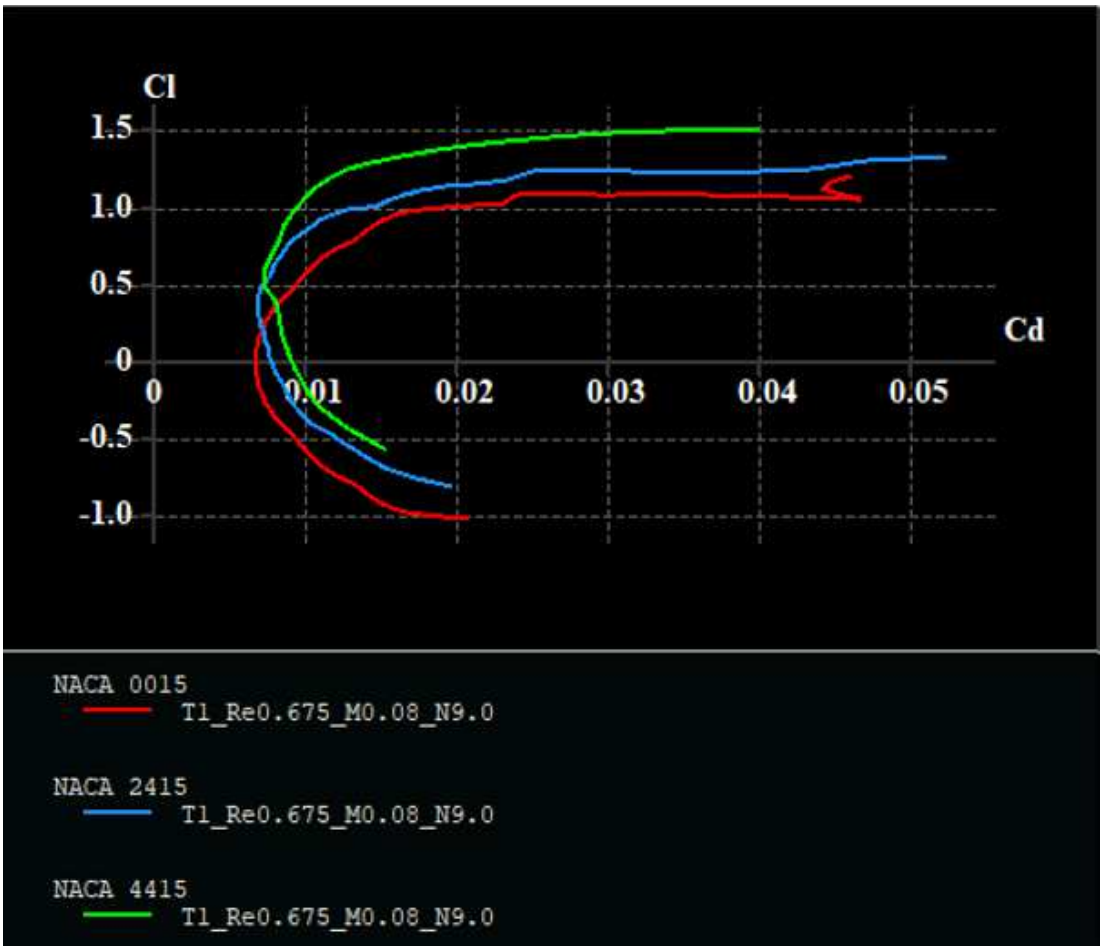

Figure 2.11: Graph of the lift coefficient C_l and Drag coefficient C_d.

The ratio of lift coefficient and drag coefficient in aircraft should be as high as possible for efficiency. According to the analysis of the XFLR5 program, the NACA4415 profile again gives the best value. With a high ratio of the lift coefficient to the drag coefficient, the aircraft will be subjected to the low drag force. Thanks to this low drag force, it will be able to increase its speed if necessary, as well as make longer flights with its existing battery.
The graph of the change in the pitching moment coefficient with a changing angle of attack is shown below.

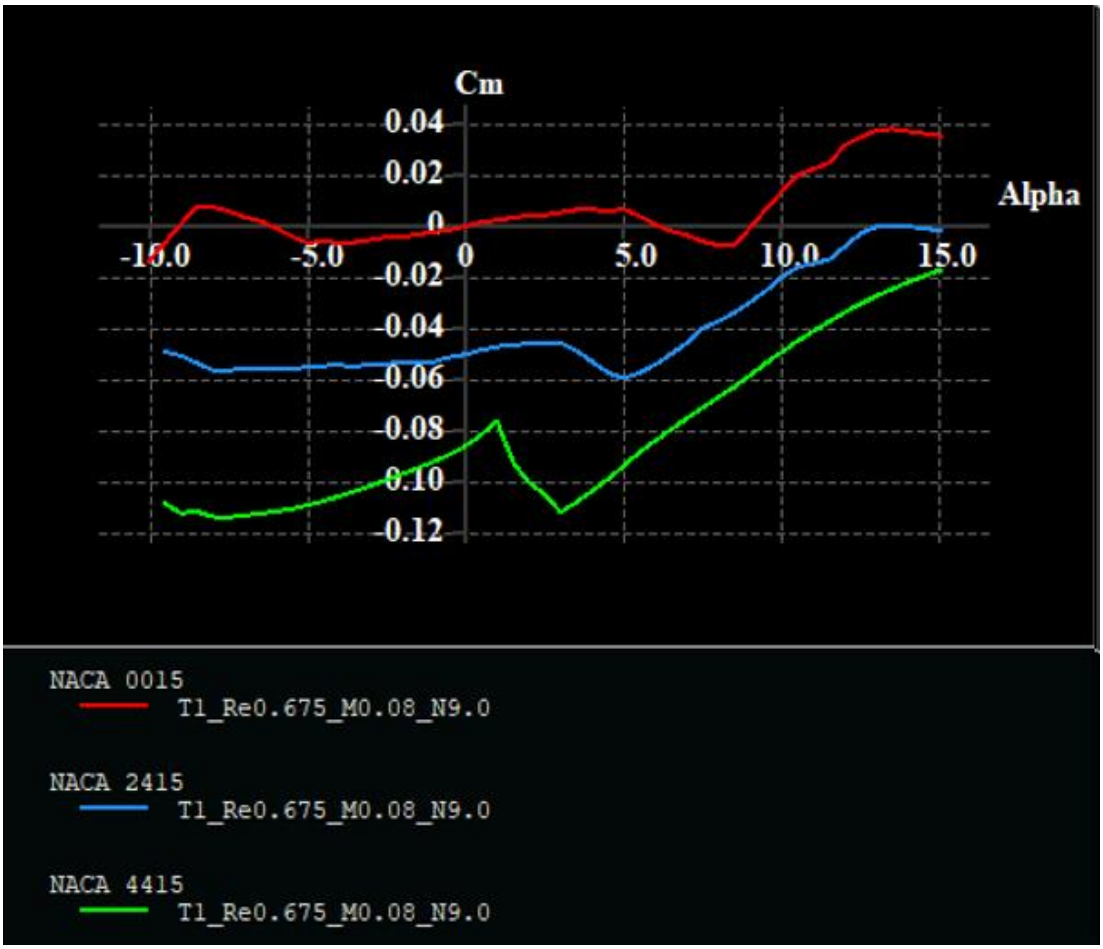

Figure 2.12: Graph of the pitching moment coefficient C_m vs Angle of attack α.

The pitching moment is one of the first parameters to be considered in the stability analysis of the aircraft. Looking at the pitching moment vs. angle of attack graph, NACA4415 was the most suitable candidate for profile selection.

3. MODELING OF THE WING

The wings of aircraft are subjected to a large number of loads during the flight. Against these loads, the wings meet their strength with their skeletons in their internal structure. The structure of this internal skeleton is the same on almost every aircraft, and it is possible to describe its elements in three subheadings. These elements are spar, rib, and shell. These elements are very effective in maintaining the aerodynamic shape. Each element provides resistance to a different load.

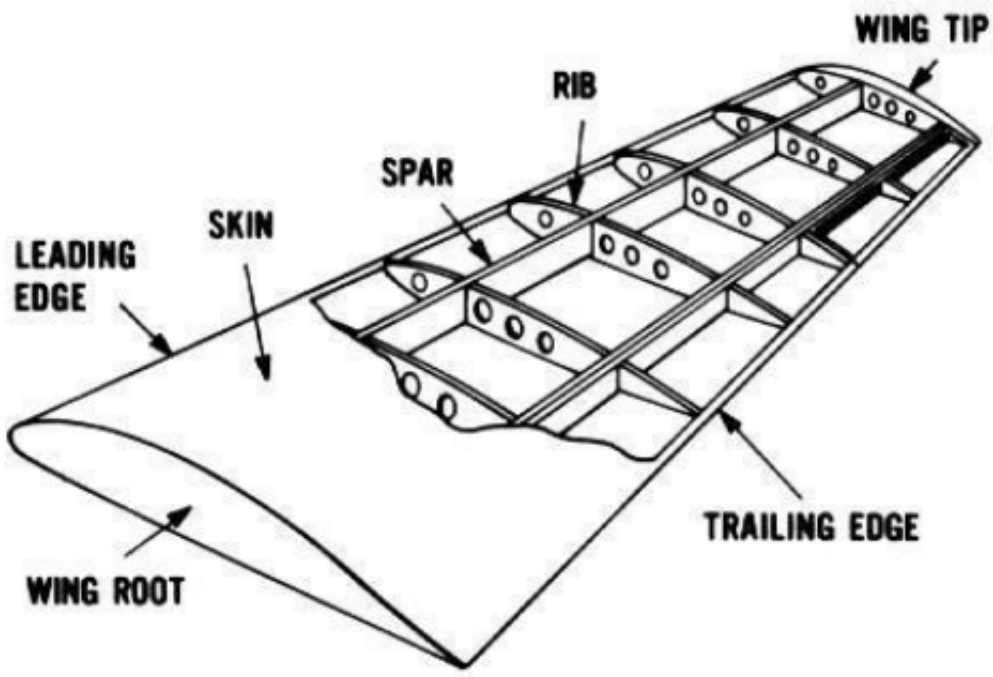

Figure 3.1: Wing Skeleton Structure Sample.

According to the parameters determined up to this section, the external design of the wing can be made. If we express the determined parameters of the wing with a table,

Table 2.1: Wing Design Parameters

Airfoil Profile	Wing Span (m)	Wing Area (m^2)	Aspect Ratio	Sweep Angle (Degree)	Dihedral Angle (Degree)	Taper Ratio	Chord Length (m)	Thickness Ratio (%)
NACA4415	1.87	0.3496	10	0	0	1	0.187	15

The necessary parameters for the external design of the wing have been calculated. As a result of the determined parameters, the top, side, and isometric views of the wing were drawn with the help of the SOLIDWORKS package program.

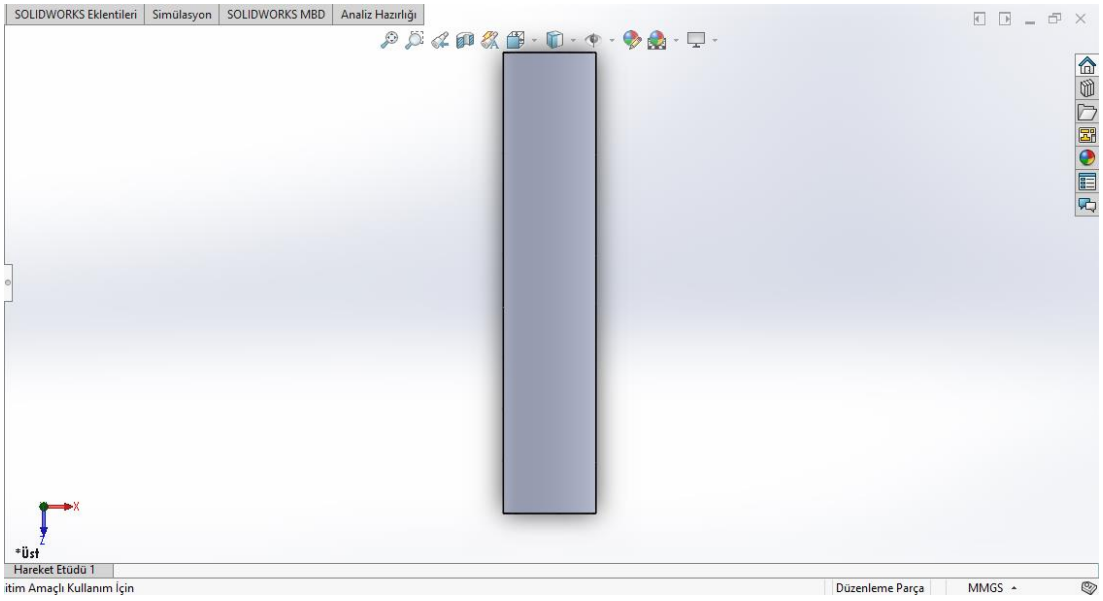

Figure 3.2: Wing Top View.

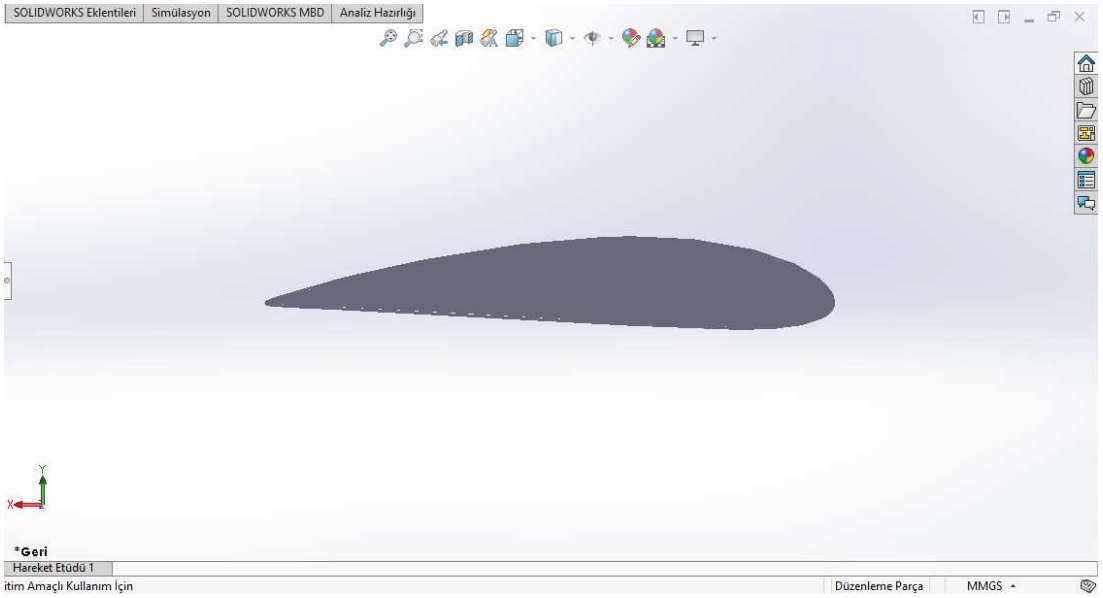

Figure 3.3: Side View of the Wing.

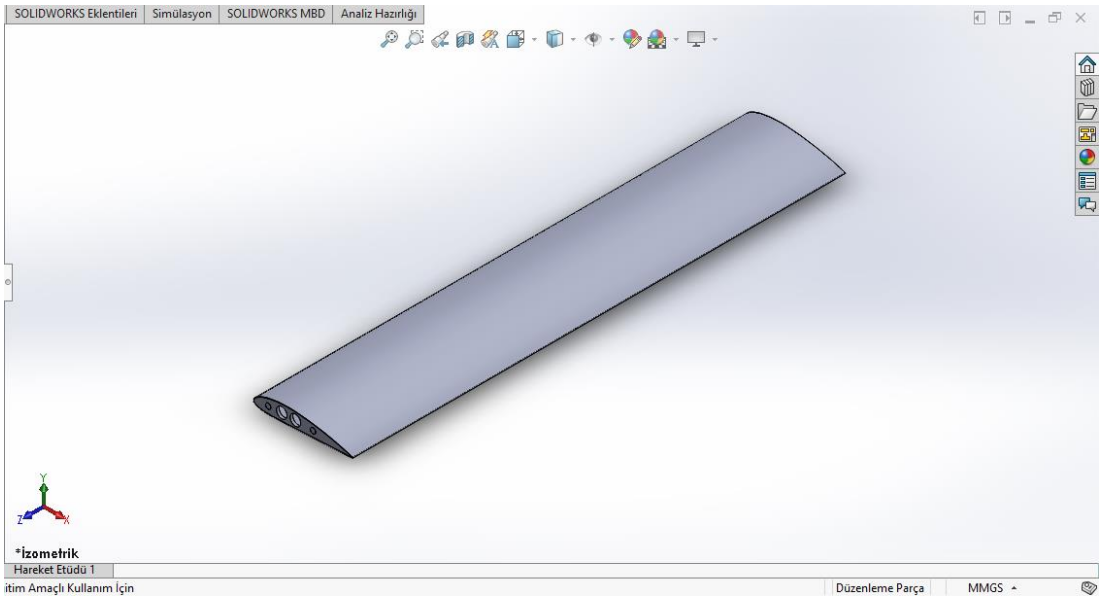

Figure 3.4: Isometric View of the Wing.

3.1 Determination of Spar Structure

3.1.1 Determination of the Number, Location, and Structure of the Spar

The spar is the primary element of the wing, which is longitudinal. Usually, the main structure that carries the load in all wing structures is the spar. The spar distributes the loads to which the wing is exposed and also ensures the transmission of loads to the fuselage. The number of spars in UAVs of today's design is often two pieces. For this reason, the number of spars in the design was determined as 2 pieces.

Resources will be used in the studies conducted on the positioning of spars. The spars should be at a certain percentage of chord length from the root of the wing to the tip, and this percentage should be between 12% and 17% for the front spar and between 55% and 60% for the rear spar.

The reason for the specified value of 55%-60% is that the 30% part is divided into control surfaces such as spoilers, ailerons, and flaps. Since the control surfaces will not be taken into account in the wing structural analysis in this study, the chord lengths at which the spars will settle were determined to be 14.5% for the front spar and 60% for the rear spar when considering future studies on the control surfaces that can be developed in the future. The positioning of the spars on the wing is given in the following SOLIDWORKS drawing.[31]

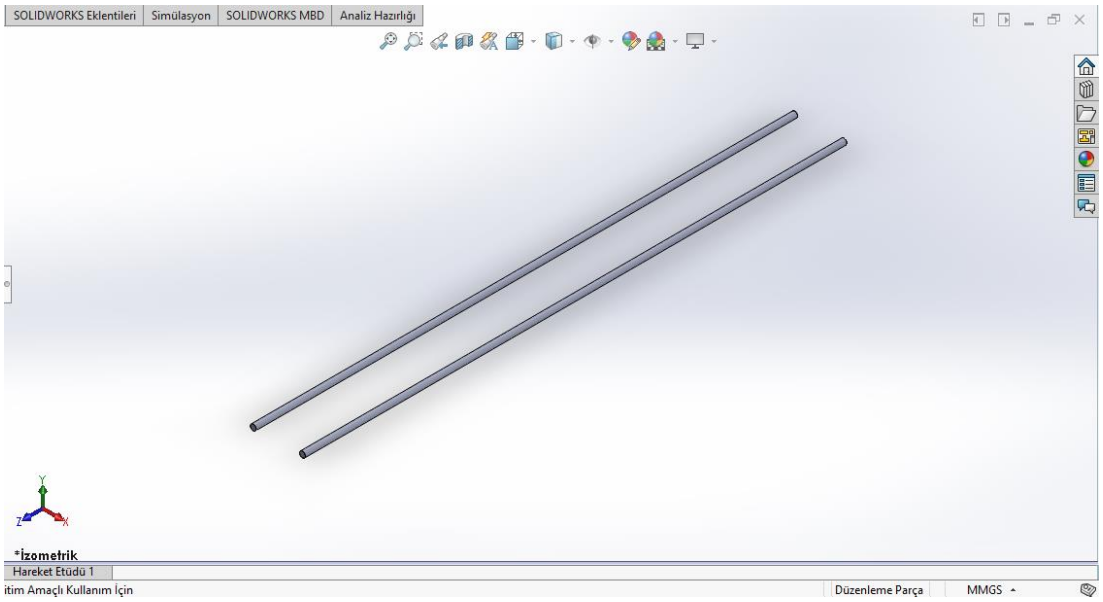

Figure 3.5: Ismoteric View of the Spar Profile

As with spar locations, ease of production takes precedence when choosing a spar profile. Although I-section profiles are the preferred type of cross-section in wing profiles in general, O-section profiles are sufficient for mini-UAVs. For this reason, the O-section profile was selected for the design.

3.2. Determination of Rib Structure

Ribs are structures that are used to distribute the loads on the wing appropriately to the spar and to maintain the aerodynamic shape of the wing, positioned at specified distances from the root of the wing to the tip and extending from the leading edge of the wing to the trailing edge. The ribs are in the form of an airfoil and are placed in parallel. At the same time, they are thin-walled structural elements that provide rigidity in the wing. By evacuating the inside of the ribs, the structural strength of the wing is increased while at the same time significant weight savings are achieved. In this study, it was deemed appropriate to design 8 ribs, including those at the root and tip of the wing. The distance between rib positions is adjusted to be equal between the 6 ribs closest to the root of the wing. The distance between the 3 ribs closest to the wing tip is also adjusted to be twice this distance. Such a solution has been achieved as a result of the decrease in structural loads acting on the structure due to the decrease in the lift force as one move towards the wingtip. Thus, ribs are more frequent in locations close to the root area

where the transport is high and the loads are higher due to this transport. Modeled image of ribs drawn in the SOLIDWORKS program and their positions are shown below.

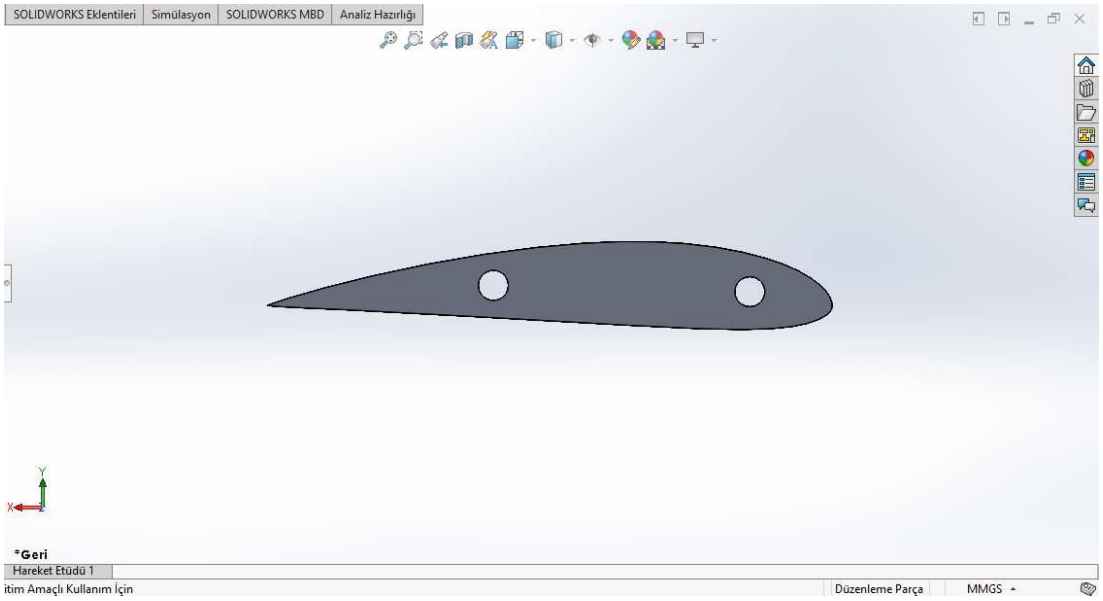

Figure 3.6: Lateral View of the Rib Structure.

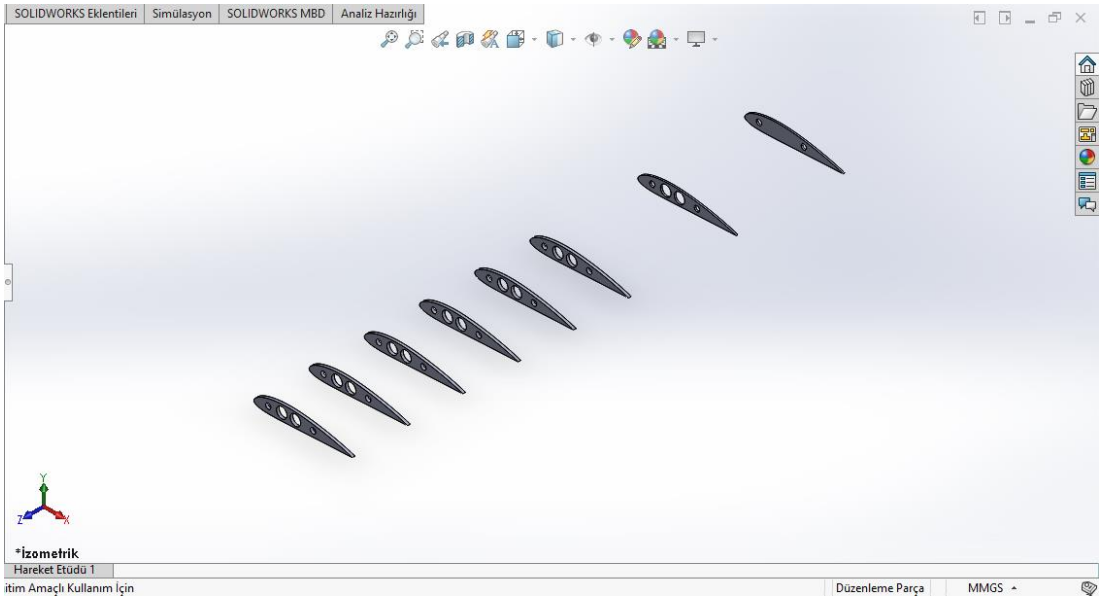

Figure 3.7: Isometric View of the Rib Structure.

3.3. Determination of Shell Structure

The shell is the first surface of the wing that comes into contact with air. The loads generated by the aerodynamic effects on the shell in interaction with the air are transferred to the ribs in the wing skeleton. The shell is very important, as it forms the overall shape of the wing. Since carbon fiber material with high mechanical properties will be preferred, it is sufficient that the shell thickness of the UAV wing being studied is 1 mm.

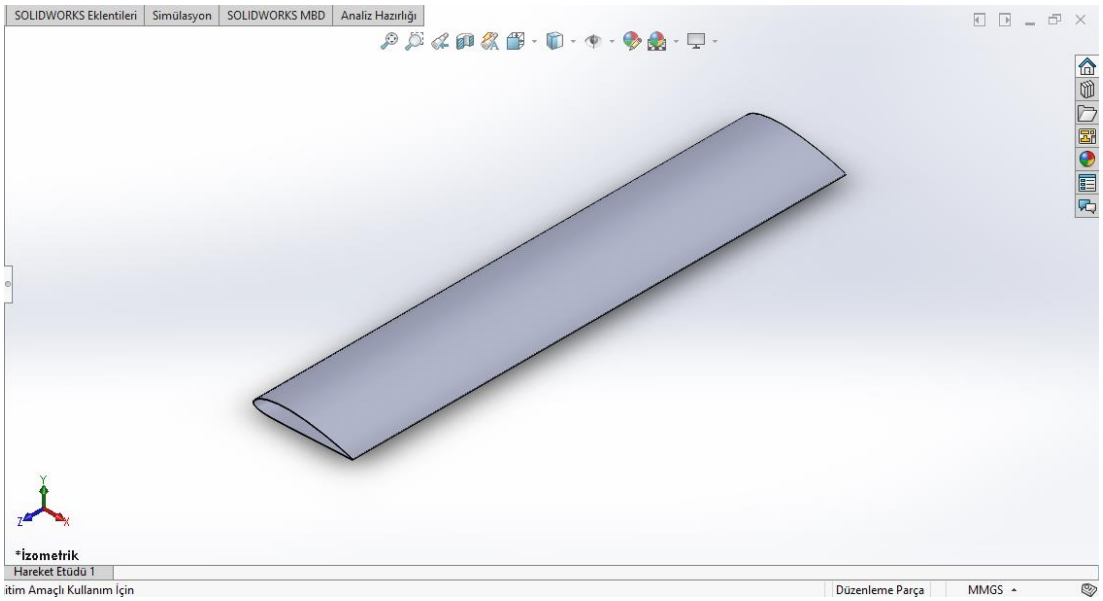

Figure 3.8: Isometric View of the Shell Structure.

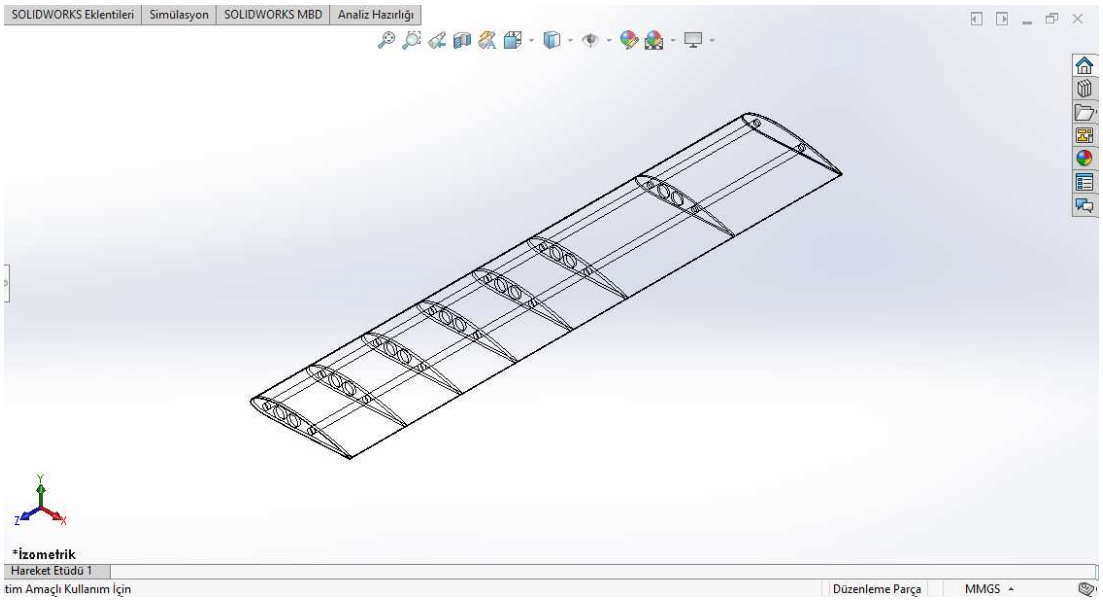

Figure 3.9: Wing Structure Designed Together with Shell, Rib, and Spar.

4. LOADS AFFECTING THE WING

4.1. Structural Loads Acting on the Wing

There are 5 basic structural loads acting on the wing of the aircraft. These loads are as indicated in the figure below; tensile, compression, torsion, shear and bending. As a result of the designs made, the wing should resist these loads and should not undergo any deformation. When it is deformed, the design is made incorrectly.

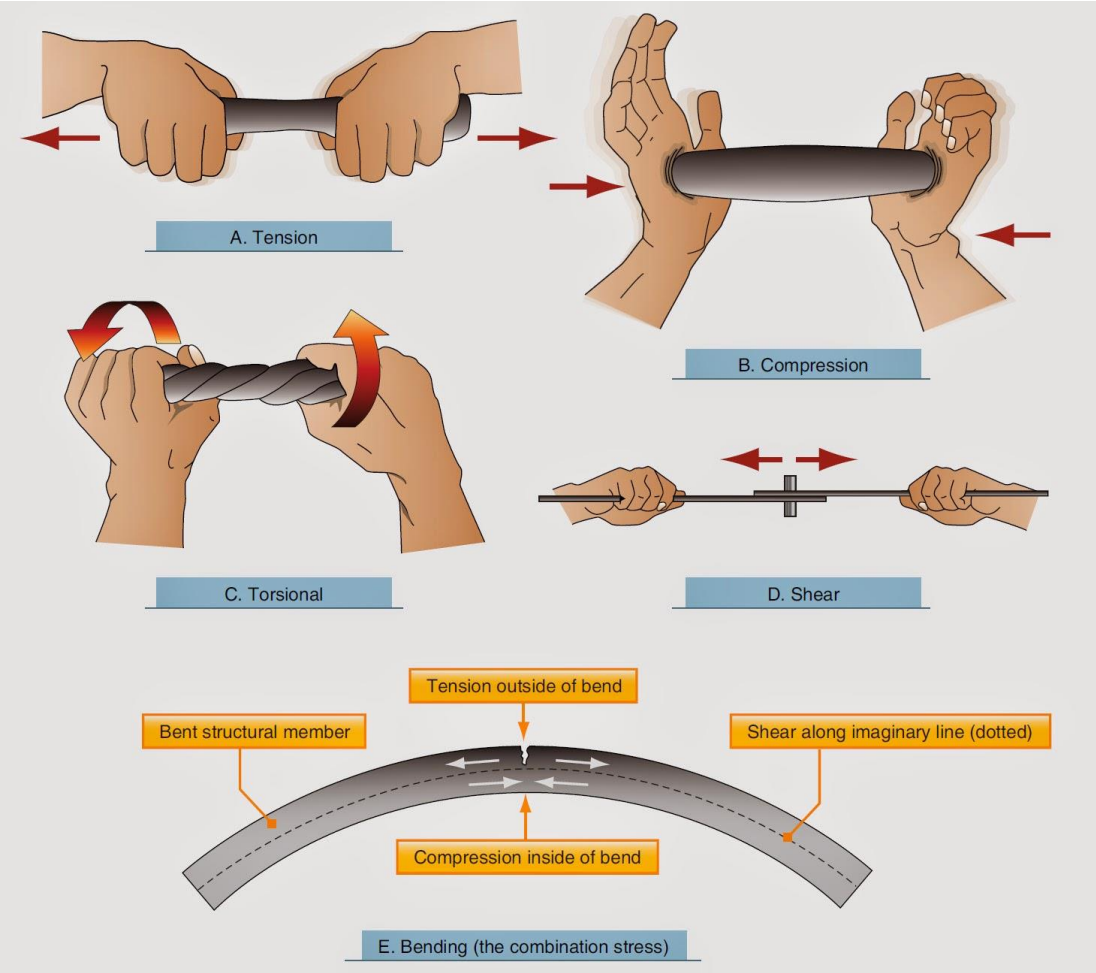

Figure 4.1: Structural Loads Acting on the Wing. [32]

4.2. Aerodynamic Loads Acting on the Wing

The loads caused by the movement of the aircraft in the airflow are aerodynamic loads. Lift and drag forces are important for the airfoil. An excess lift force makes a positive contribution to the design, while an excess drag force makes a negative contribution to the design. In the profile selections made in the previous sections, the NACA4415 profile with the highest lift coefficient was selected. It is expected that the lift force that the selected wing profile will create will be such that it will lift the weight of the aircraft in the opposite direction during the cruise flight. These analyses will be carried out numerically in the following sections.

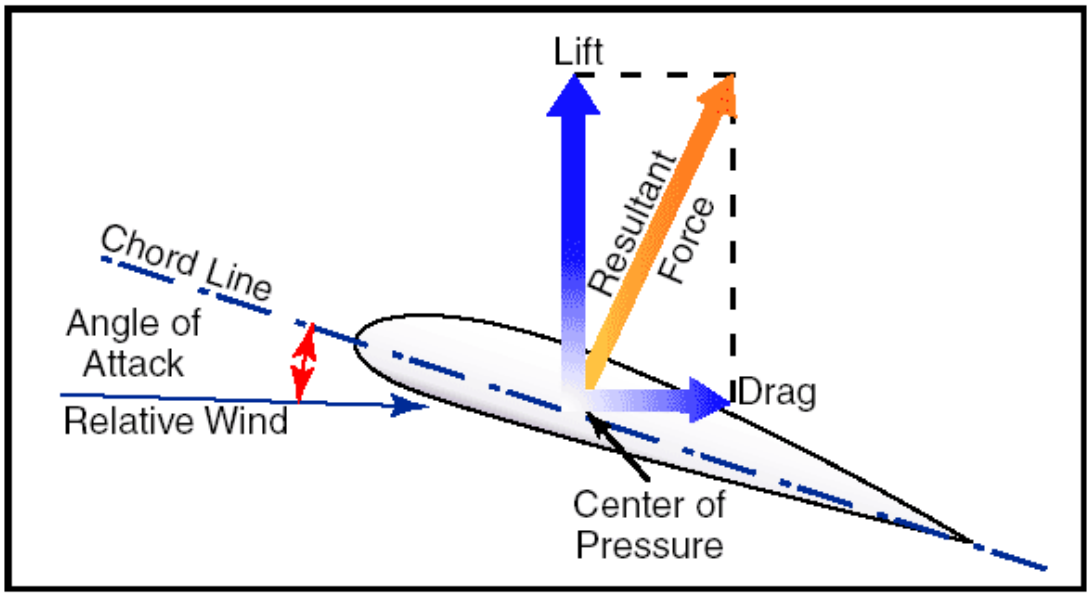

Figure 4.2: Aerodynamic Force Vectors on An Airfoil.

4.2.1 Safety Factor

In aviation, one of the most important parameters of a design is safety. Safety is the most important criterion since people are generally transported. For this reason, the safety factor is used in design calculations for unexpected situations and loadings. While this value is between 1.25 and 1.5 in commercial aircraft, it is between 1 and 1.25 in UAV-type aircraft. Since the design is not an attack-type UAV, the safety factor can be chosen as 1 for future calculations.[30]

4.2.2. Load Factor

In addition to producing a lift force at least as much as the weight of the aircraft in level flight, the aircraft should also be able to create a lift force as much as the loads on the aircraft in the maneuvers to be made. During maneuvers, the aircraft is loaded more than normal. We can express the load factor as the ratio of the lift produced by the aircraft to the weight of the aircraft. The load factor of an airplane in level flight is taken as 1. The load factor of aircraft can be determined from V-n diagrams.

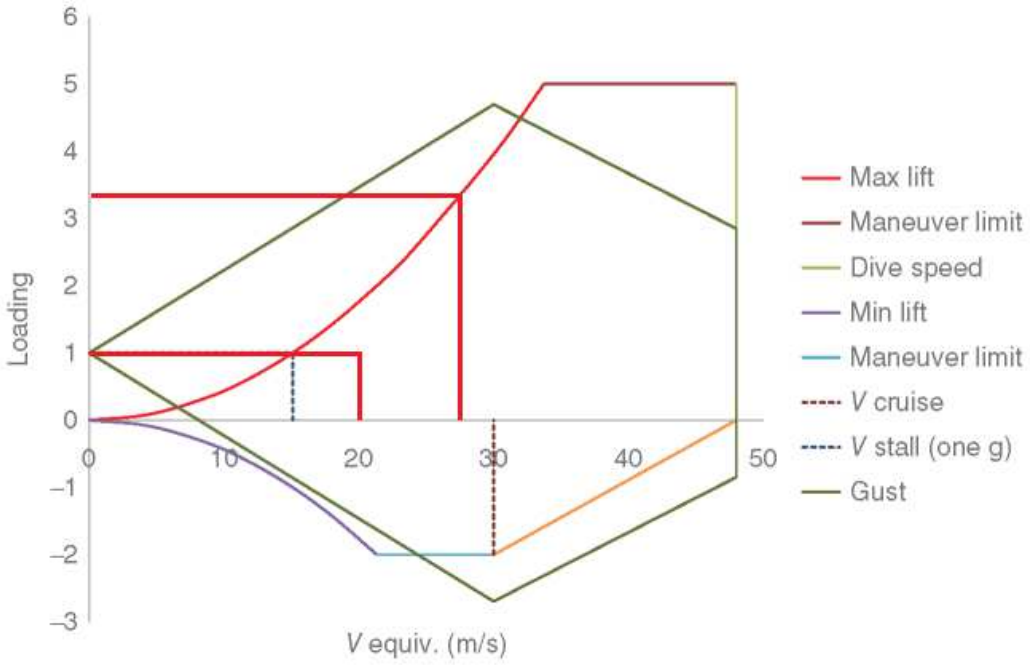

Figure 4.3: V-n Diagram. [33]

When looking at the V-n diagram, it is taken as 3.24, which corresponds to our maximum speed of 27.7472 m/s. This value is more than sufficient for both reconnaissance and suicide missions. The higher the load factor is, the higher the calculated value for the maximum load that will affect the wing. Therefore, the lift force required by the wing should be just as much.

4.3. Calculation of the Lift Force Required

$$L = Lift\ Force\ (N)$$

$$\rho = Density\ of\ Air\ (\frac{kg}{m^3})$$

$$V = Velocity\ (m/s)$$

$$S = Wing\ Area\ (m^2)$$

$$C_l = Lift\ Coefficent$$

$$L = \frac{1}{2} * \rho * V^2 * S * C_l$$

$$L_{cruising} = \frac{1}{2} * \rho_{1443.24ft} * V^2_{cruise} * S * C_{l_0}$$

$$= (\frac{1}{2}) * \left(1.1750 \frac{kg}{m^3}\right) * (20.3666 m/s)^2 * (0.3496 m^2) * (0.414)$$

$$= 35.2802\ N$$

$$L_{max} = \frac{1}{2} * \rho_{9030.39ft} * V_{max}^2 * S * C_{l_{max}}$$

$$= (\frac{1}{2}) * \left(0.7980 \frac{kg}{m^3}\right) * (27.7472 m/s)^2 * (0.3496 m^2) * (1.5)$$

$$= 161.0922\ N$$

4.4. Calculation of the Maximum Load

Maximum Load = W_0 *n*FS*

MTOW = Maximum Take-off Weight (kg)

W_0 *= Maximum Take-off Weight (N)*

n = Load Factor

FS =Factor of Safety

$$Maximum\ Load_{cruising} = (4.86kg) * \left(\frac{9.8066m}{s^2}\right) * (1) * (1) = 47.6603N$$

Since 47.6603 is greater than 35.2802 the average MTOW value obtained should be reduced in order to the lift force that can balance the load.

$$Maximum\ Load_{cruising} = (3.59kg) * \left(\frac{9.8066m}{s^2}\right) * (1) * (1) = 35.2802\ N$$

The revised MTOW is 3.59 kg.

$$Maximum\ Load_{maneuvering} = (3.59kg) * \left(\frac{9.8066m}{s^2}\right) * (1) * (3) = 105.8406\ N$$

According to the calculated values,

Table 3.1: Maximum Load and Lift Forces

Maximum Load		Lift Force	
Cruising	Maneuvering	Cruising	Maneuvering
35.2802 N	105.8406 N	35.2802 N	161.0922 N

As can be seen from the table, the aircraft can create the required lift force both during level flight and during maneuvering. Accordingly, it has been observed that the arithmetic average of the MTOW values of the reference UAVs is higher for sufficient lift force load balance. This value has been revised according to these analyses.

4.4.1. Empty Weight Calculation

The MTOW value of the aircraft was determined by the steps made in the previous sections. Using this value, the calculation of the empty weight of the aircraft can be calculated with the help of the table below. [26] After calculating the empty weight, the parts that will make up the empty weight will be allocated to the camera system and/or light warhead weight.

Table 4.1: Empty Weight Fraction with W_0.

$W_e/W_0 = A W_0^C K_{vs}$	A	C
Sailplane—unpowered	0.86	−0.05
Sailplane—powered	0.91	−0.05
Homebuilt—metal/wood	1.19	−0.09
Homebuilt—composite	0.99	−0.09
General aviation—single engine	2.36	−0.18
General aviation—twin engine	1.51	−0.10
Agricultural aircraft	0.74	−0.03
Twin turboprop	0.96	−0.05
Flying boat	1.09	−0.05
Jet trainer	1.59	−0.10
Jet fighter	2.34	−0.13
Military cargo/bomber	0.93	−0.07
Jet transport	1.02	−0.06

K_{vs} = variable sweep constant = 1.04 if variable sweep
= 1.00 if fixed sweep

W_0 = *Maximum Take-off Weight (kg)*

W_e = *Empty Weight (kg)*

$$\frac{W_e}{W_0} = (A) * (W_0)^C * (K_{vs}) = (0.99) * (3.59kg)^{-0.09} * (1.00) = 0.8824$$

$$W_e = (3.59kg) * (0.8824) = 3.16\ kg$$

4.4.2 Weight Calculation of the Camera System and the Warhead

As a result of the calculations, the MTOW value was calculated as 3.59 kg. Curb weight is 3.16kg. Payload weight, which is the difference, will be used as 0.42 kg for the camera system and/or warhead. In the literature research, it has been observed that the camera systems and warhead weights of the UAVs that are currently produced and used are much lower than 0.42 kg.

5. ANALYSIS

While applying this method, there are various critical details for the accuracy of the result to approach the truth. The multiplicity of the number of elements and nodes will increase the accuracy of the analysis because the transmission of loads between elements will be healthier. In addition, keeping the number of meshes as high as possible in the regions that are critical for loading will increase the accuracy of the analysis.

5.1. Static Analysis of the Designed Wing

5.1.1. Analysis with the Finite Element Method

The finite element method (FEM) is a mathematical solution method that engineers use to obtain results as close to reality as possible in their studies and the problems they are trying to solve. Later, numerical analysis of the physical problem modeled by this mathematical method is performed with finite element analysis (FEA). This system is a model that can be subdivided and has material properties and boundary conditions. The finite element method is to solve a complex problem by simplifying it. For this purpose, the geometry on which the calculation will be made is divided into many, small and simple, sub-regions called finite elements. Thus, instead of making difficult solutions on complex and large geometry, simpler solutions can be made at nodal points on smaller and simple finite elements. Patran is the world's most widely used pre/post-processing software for Finite Element Analysis (FEA), providing solid modeling, meshing, analysis setup, and post-processing for multiple solvers including MSC Nastran, Marc, Abaqus, LS-DYNA, ANSYS, and Pam-Crash. Patran provides a rich set of tools that streamline the creation of analysis-ready models for linear, nonlinear, explicit

dynamics, thermal, and other finite element solutions. From geometry cleanup tools that make it easy for engineers to deal with gaps and slivers in CAD to solid modeling tools that enable the creation of models from scratch, Patran makes it easy for anyone to create FE models. Meshes are easily created on surfaces and solids alike using fully automated meshing routines, manual methods that provide more control, or combinations of both. Finally, loads, boundary conditions, and analysis setup for most popular FE solvers are built-in, minimizing the need to edit input decks. Patran's comprehensive and industry-tested capabilities ensure that your virtual prototyping efforts provide results fast so that you can evaluate product performance against requirements and optimize your designs. [34]

MSC Nastran is a multidisciplinary structural analysis application used by engineers to perform static, dynamic, and thermal analysis across the linear and nonlinear domains, complemented with automated structural optimization and award winning embedded fatigue analysis technologies, all enabled by high-performance computing. Engineers use MSC Nastran to ensure structural systems have the necessary strength, stiffness, and life to preclude failure (excess stresses, resonance, buckling, or detrimental deformations) that may compromise structural function and safety. MSC Nastran is also used to improve the economy and passenger comfort of structural designs. Manufacturers leverage MSC Nastran’s unique multidisciplinary approach to structural analysis at various points in the product development process. MSC Nastran may be used to:

Virtually prototype early in the design process, saving costs traditionally associated with physical prototyping,

Remedy structural issues that may occur during a product’s service, reducing downtime and costs,

Optimize the performance of existing designs or develop unique product differentiators, leading to industry advantages over competitors. MSC Nastran is based on sophisticated numerical methods, the most prominent being the Finite Element Method. Nonlinear FE problems may be solved with built-in implicit numerical techniques. A number of optimization algorithms are available, including MSCADS and IPOPT. The fatigue capability in MSC Nastran uses CAEfatigue, the fastest and most robust fatigue solution on the market today. [35]

Static analysis allows us to observe important results about wing strength and lift by examining the deformation, von-mises stresses, and reaction forces that will occur in the wing.

5.1.2. Determining the Lift Distribution on the Wing

In the previous sections, the lift force required by the wing during maneuvering flight was calculated as 161.0922 N. In this context, it will be calculated how the 161.0922 Newtonian lift acting on the wing is distributed on the wing. As a result of this calculation, a value of 161.1871 N was obtained, which is very close to the value calculated by hand calculation using the XFLR5 program.

Table 5.1: Detailed Lift Distribution On The Wing.

Delta Lift (N)	Coordinate (mm)	Rib No	Distance to Root (m)	Resultant Force (N)	Delta Lift (N)	Coordinate (mm)
0,1730	-934,3593	1	0,0025	4,7612	4,7612	24,4671
0,0675	-931,7983				4,7444	73,3341
0,1615	-926,6833	2	0,1073	9,4552	4,7108	122,0002
0,2921	-919,0283				4,6604	170,3318
0,4552	-908,8543	3	0,2121	9,2538	4,5934	218,1966
0,6462	-896,1892				4,5099	265,4633
0,8599	-881,0678				4,4100	312,0025
1,0912	-863,5314	4	0,3169	13,2139	4,2940	357,6864
1,3349	-843,6281				4,1621	402,3899
1,5865	-821,4124	5	0,4217	8,1766	4,0146	445,9906
1,8417	-796,9454				3,8519	488,3687
2,0969	-770,2939				3,6746	529,4084
2,3488	-741,5312				3,4832	568,9969
2,5949	-710,7359	6	0,5265	14,2881	3,2785	607,0258
2,8330	-677,9926				3,0614	643,3910
3,0614	-643,3910				2,8330	677,9926
3,2785	-607,0258				2,5949	710,7359
3,4832	-568,9969				2,3488	741,5312
3,6746	-529,4084				2,0969	770,2939
3,8519	-488,3687				1,8417	796,9454
4,0146	-445,9906	7	0,7302	16,3633	1,5865	821,4124
4,1621	-402,3899				1,3349	843,6281
4,2940	-357,6864				1,0912	863,5314
4,4100	-312,0025				0,8599	881,0678
4,5099	-265,4633				0,6462	896,1892
4,5934	-218,1966				0,4552	908,8543
4,6604	-170,3318				0,2921	919,0283
4,7108	-122,0002				0,1615	926,6833
4,7444	-73,3341				0,0675	931,7983
4,7612	-24,4671	8	0,9329	5,0814	0,1730	934,3593
		One Wing		80,5936		
		Whole Wing		161,1871		

The values given above have been tabulated by making a resultant calculation for the areas affected by each rib. The graph of the lift distribution curve along the wing length was created with the help of the Microsoft Excel Program. By looking at the graph, it is possible to see that this distribution resembles an elliptic curve and to say that the calculations are correct.

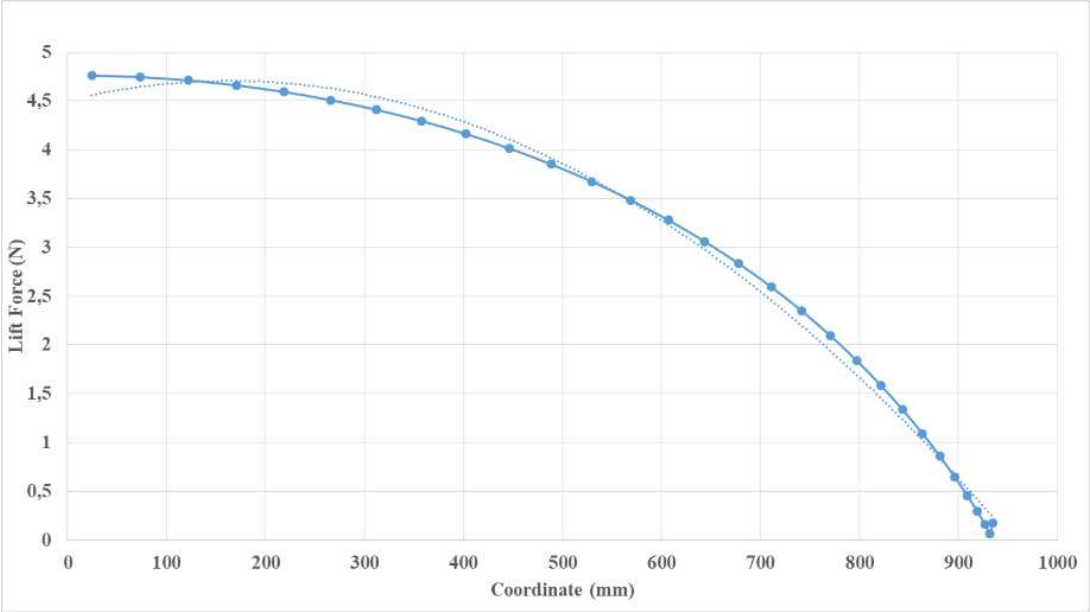

Figure 5.1: Lift Distribution over One Wing.

By defining fixed support at the root of the wing, the resultant lift forces obtained as a result of the wing analysis in the XFLR5 program were applied on the rib to the points at a quarter beam distance from the leading edge point, which is the aerodynamic center point.

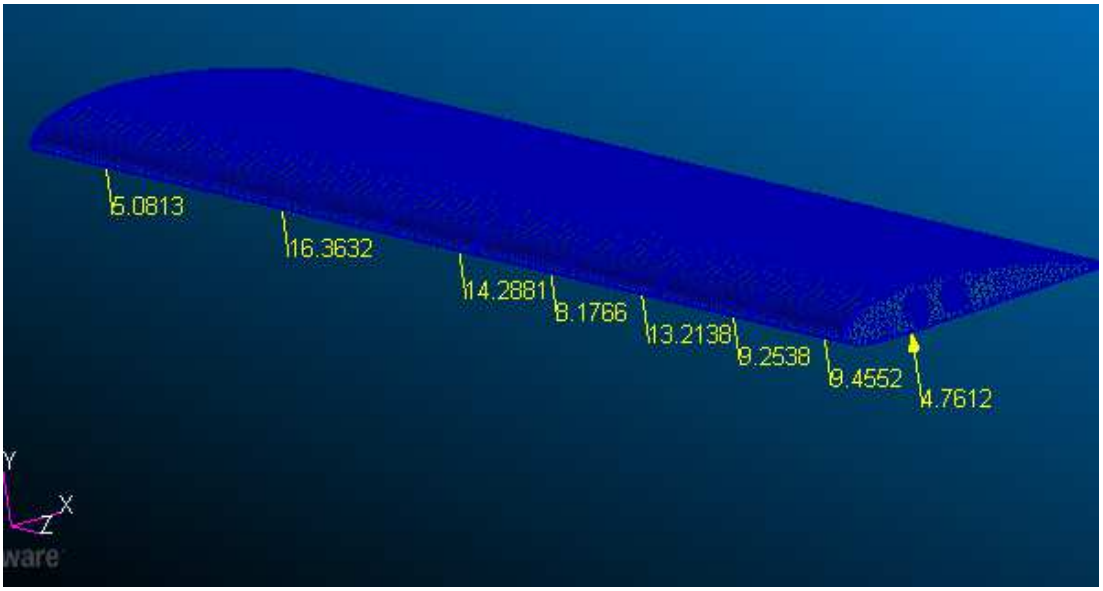

Figure 5.2: Lift Force Distribution over Ribs.

5.1.3. Creating Mesh Network

Since the thicknesses of the elements such as spar, rib, shell, which form the endoskeleton structure of the wing in this graduation project, will be very small compared to their lengths, 2D analysis was used for this study. In the figures given below, elements simulating 2D mesh structures are Quad element shape, Isomesh mesher, and Quad4 for the shell; Tet element shape, Tetmesh mesher, and Tet10 for spars and ribs are created with smaller and more precise values than the mesh value automatically calculated by the program. Care has been taken to ensure that the aspect ratio of meshes does not exceed 3.

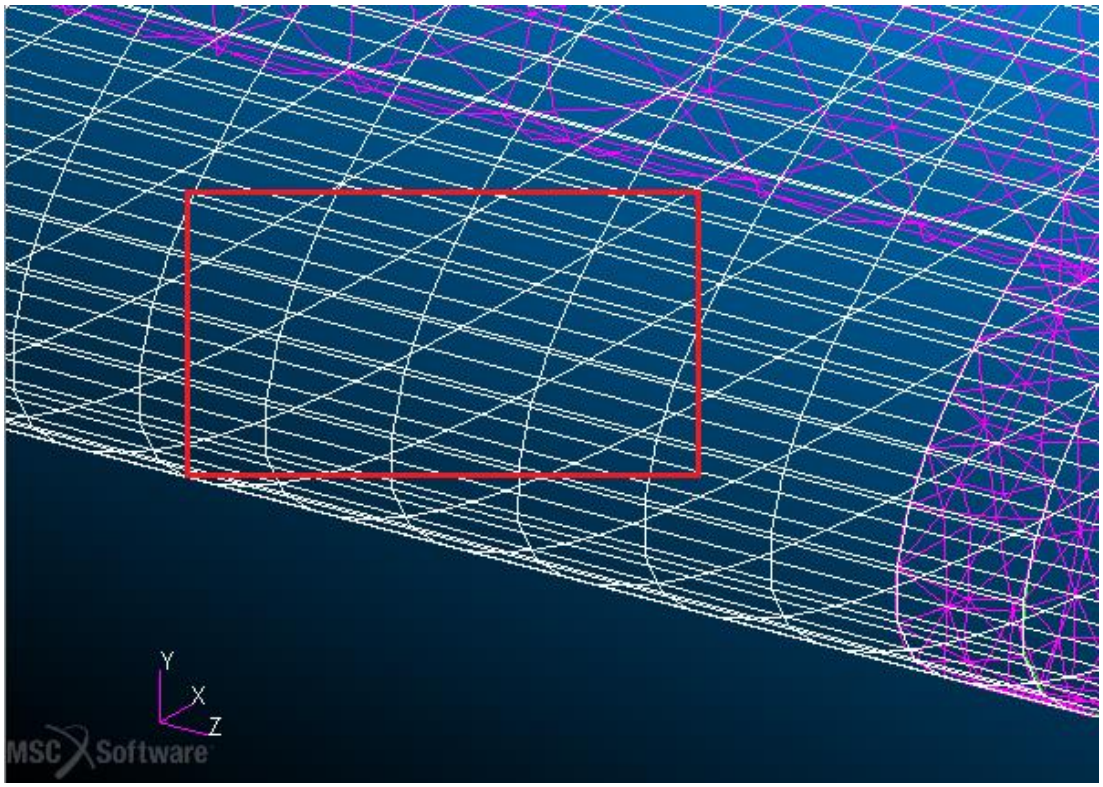

Figure 5.3: Mesh Network for Shell.

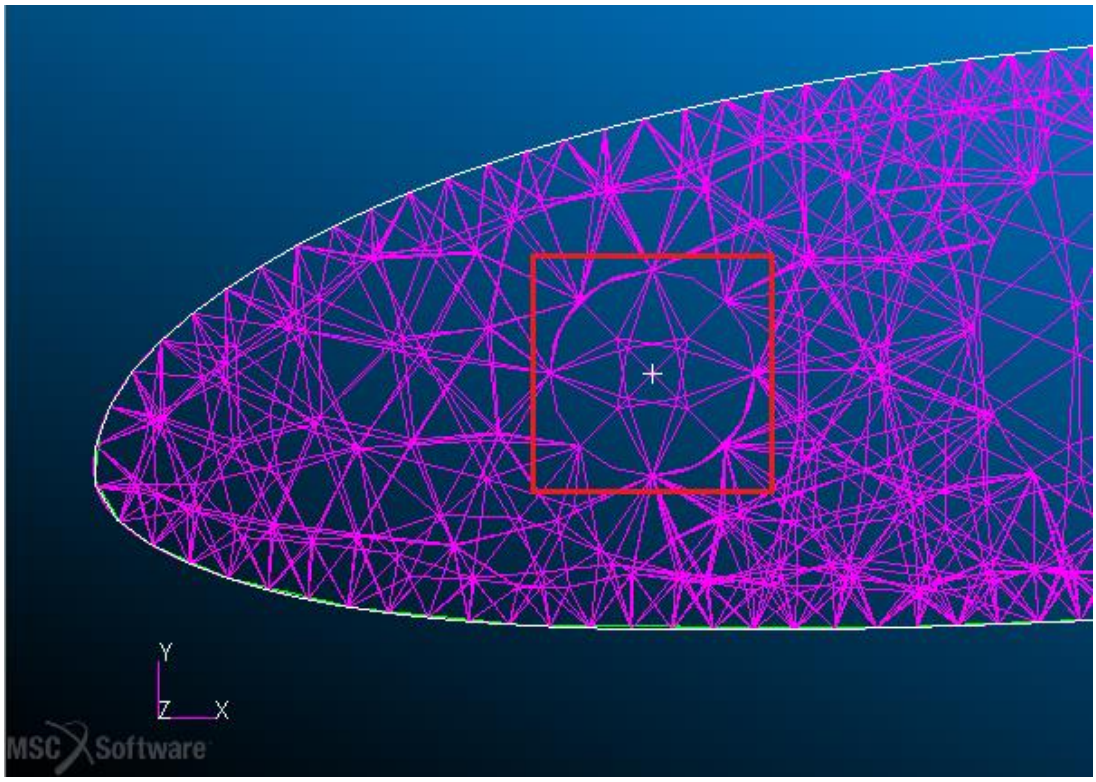

Figure 5.4: Mesh Network for Spars.

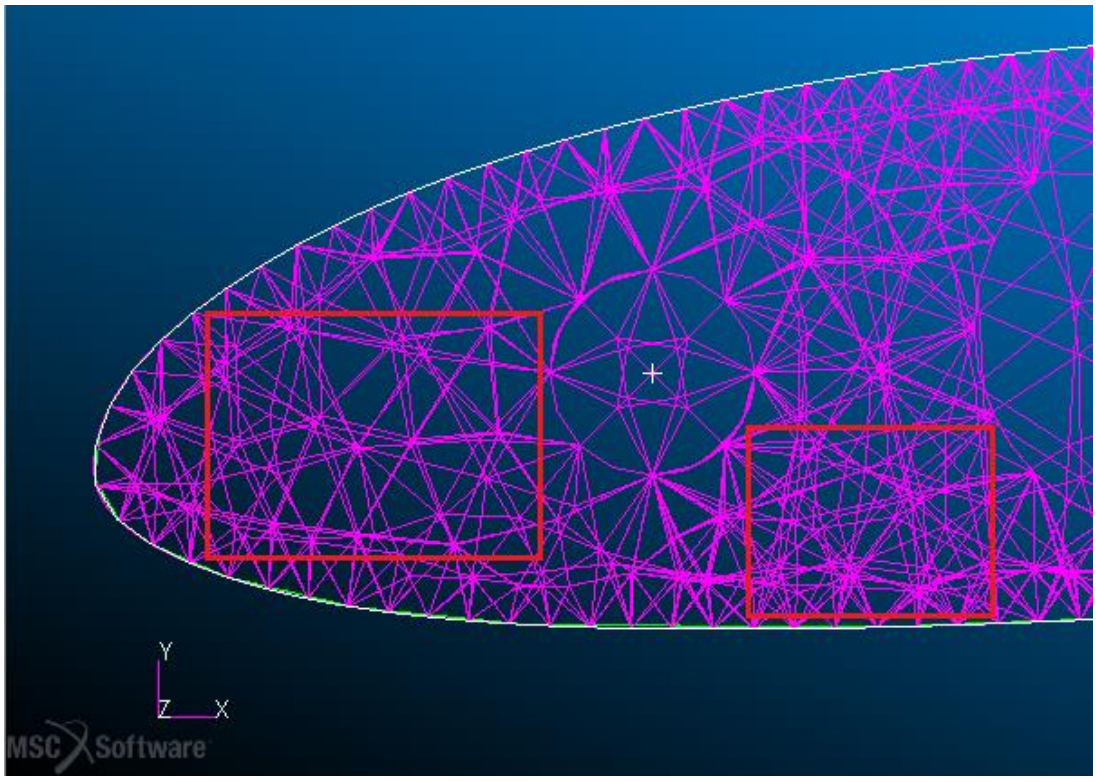

Figure 5.5: Mesh Network for Ribs

5.1.4. Wing Material Selection

In order to get quick results, all parts of the wing are defined as carbon fiber material in the database of the MSC PATRAN/NASTRAN program. This composite material can withstand very high stresses in the GPa range and at the same time, it provides a significant weight advantage due to its lightness.

While choosing the material of the wing, the usage rates in aviation were investigated and the material was selected accordingly. CFRP was chosen as the wing material by keeping the material cost in the second place since it will be studied on the mini UAV due to its high strength and ultra-lightness by advancing with the optimization logic. While CFRP can withstand very high stresses, low strain values are achieved. The properties of the material used are shown below. [36]

Table 5.2: Carbon Fiber Material Properties.

Property	Unit	Value
Density of CFRP	kg/m^3	1544
Hardness (Rockwell)	HRB	62–67
Density of carbon fiber	kg/m^3	1800
Density of epoxy matrix	kg/m^3	1200
Elastic modulus of carbon fiber	GPa	230
Elastic modulus of epoxy matrix	GPa	4.5
Tensile strength of carbon fiber	GPa	5
Tensile strength of epoxy matrix	MPa	130
Poisson's ratio of carbon fiber	–	0.3
Poisson's ratio of epoxy matrix	–	0.4
Fracture toughness of carbon fiber (energy/G_c)	J/m^2	2
Fracture toughness of epoxy matrix (energy/G_c)	J/m^2	500

CFRP: carbon fiber–reinforced plastic.

5.1.5 Thickness of Wing Elements

The thicknesses of the wing elements, whose material information above are given, were determined on the wing and are given in the table below. Since the loading at the root of the wing will be higher, the thickness of the first 6 ribs was determined as 5 mm, while the thickness of the other 2 ribs was determined as 3 mm in order to remove this loading. The diameter of the spars is 5 mm, the diameter of the rib holes providing the transition between the ribs is 10 mm and the shell thickness is 1 mm.

REFERENCES

[1] https://baykartech.com/tr/uav/bayraktar-mini-iha/

[2] https://www.stm.com.tr/uploads/docs/1628857620_taktikminiihasistemleri.pdf?

[3] https://www.aselsan.com.tr/MIUS_Mini_Insansiz_Ucan_Sistem_7178.pdf

[4]http://www.globalteknik.com.tr/default.asp?dil=eng&kkk=gurupaciklama&id=24&resim=&altID=21&anaadi=Air%20Platform

[5] https://avia-pro.net/blog/tai-keklik-tehnicheskie-harakteristiki-foto

[6] https://militaryleak.com/2019/03/19/ram-high-precision-loitering-uav/

[7] https://res2.weblium.site/res/5dfe007809892000216e9925/5e3c78888cf2ee0021b310a1

[8] http://ukrinmash.com/uploads/files/5909e14c6e385.pdf

[9] https://athlonavia.com/en/furia/

[10] https://www.appliedaeronautics.com/albatross-uav

[11] https://www.homelandsecurity-technology.com/projects/skate-small-unmanned-aerial-system-suas/

[12] https://www.avinc.com/tms/switchblade

[13] https://www.avinc.com/images/uploads/product_docs/Raven_Datasheet_v1.1.pdf

[14] https://www.designation-systems.net/dusrm/app2/q-14.html

[15] https://www.lockheedmartin.com/content/dam/lockheed-martin/rms/documents/desert-hawk/Desert_Hawk_Brochure.pdf

[16] https://elbitsystems.com/products/uas/skylark-i-lex/

[17] https://www.israeli-weapons.com/weapons/aircraft/uav/skylark_r/Skylark.html

[18] http://www.topoequipos.com/topoequipos2.0/drones/avian-s-real-time-surveillance

[19] https://avia-pro.net/blog/pteryx-tehnicheskie-harakteristiki-foto

[20] https://fccid.io/ANATEL/03185-16-09155/Manual-do-LA/63A46470-9790-421D-B88A-D1155AE4CF2A/PDF

[21] https://www.survey-copter.com/wp-content/uploads/2014/04/UAS12_Tracker-en.pdf

[22] https://www.army-technology.com/projects/emt-aladin-uav/

[23]https://www.topconpositioning.com/sites/default/files/product_files/sirius_solutions_catalog_7010_2162_revb_sm_0.pdf

[24] https://zala-aero.com/en/production/bvs/zala-421-08m/

[25] https://zala-aero.com/en/production/bvs/zala-421-16e2/

[26] **Raymer, D. P.** (1992). *Aircraft Design: A Conceptual Approach.* Washington, DC: American Institute of Aeronautics and Astronautics (AIAA).

[27] http://airfoiltools.com.

[28] **Kontogiannis S. G. & Ekaterinaris J. A.** (2013). Design, performance evoluation and optimization of a UAV. *Aerospace Science and Technology. 29*(2013),341. doi: https://doi.org/10.1016/j.ast.2013.04.005.

[29] **Güzelbey ve Eraslan ve Doğru**, Effects of Taper Ratio on Aircraft Wing Aerodynamic Parameters. Gaziantep University, Turkey.

https://dergipark.org.tr/tr/download/article-file/629766.

[30] **Acar,H (2018) ,** *Principle of Aircraft Desing Lecture Notes.*

[31] **Niu, C.** (2002). Airframe structural design: Practical design information and data on aircraft structures. Hong Kong: Conmilit Press.

[32] https://nanopdf.com/download/chapter-4-aircraft-basic-construction_pdf.

[33] https://ebrary.net/59626/engineering/preliminary_structural_analysis.

[34] https://www.mscsoftware.com/product/patran.

[35] https://www.mscsoftware.com/product/msc-nastran.

[36] https://www.semanticscholar.org/paper/Surface-grinding-of-carbon-fiber–reinforced-plastic-Wang-Ning/6d2a18bfebf6acaf523987b370714b54869ace3e/figure/.